J. Fluid Mech. (2003), *vol.* 488, *pp.* 245–282.
DOI: 10.1017/S0022112003004889 Printed in the United Kingdom

Quasi-modes in boundary-layer-type flows. Part 2. Large-time asymptotics of broadband inviscid small-amplitude two-dimensional perturbations

By IGOR A. SAZONOV[1]† AND VICTOR I. SHRIRA[2]

[1]Department of Applied Mathematics, University College Cork, Cork, Ireland

[2]Department of Mathematics, Keele University, Keele ST5 5BG, UK
v.i.shrira@keele.ac.uk

(Received 12 August 2002 and in revised form 23 December 2002)

The paper is the second in a series concerned with the development of the quasi-mode concept in the context of boundary layers. The evolution of localized two-dimensional perturbations in boundary layers without inflection points is considered within the framework of linear inviscid theory. Making use of the results of Part 1 (Shrira & Sazonov 2001) for monochromatic perturbations it is shown that arbitrary broadband initial perturbations tend to a universal asymptotic regime at large times t. We refer to the phenomenon of the emergence of the asymptotic regime as 'adjustment'. The regime itself corresponds to a slow dynamics of long-wave triple-deck-type perturbations and is described well as the evolution of a single quasi-mode, which allows dramatic simplification of its description. At the asymptotic stage the spatio-temporal structure of the perturbation is explicitly described in terms of Fresnel's functions with coefficients specified by certain integrals of the initial distribution. Asymptotically the perturbation represents a sharply localized group of decaying oscillations which propagate with celerity approaching the mean flow velocity at the surface. For generic perturbations, the decay, in terms of streamwise velocity, is $t^{-1/2}$. The envelope of the group is formed by the Landau damping intrinsic to the quasi-modes, and the length of the group and the number of oscillations in the group grow with time as $t^{2/3}$ and $t^{1/6}$, respectively. The evolution of the non-quasi-modal part is also investigated. The vorticity perturbation is found to form a vortex patch shaped like a comet tail and advected by the mean flow. The picture of evolution established for generic perturbations is found to hold for several classes of non-generic but physically relevant initial distributions; the corresponding solutions are presented and discussed. The analytical results have been confirmed by the direct numerical simulation of the linearized primitive equations.

1. Introduction

During most of the 20th century theoretical studies of the evolution of perturbations in boundary-layer-type flows were dominated by the normal-mode analysis and the search for linearly unstable modes, the latter being viewed as the main and

† Present address: School of Engineering, University of Wales Swansea, Singleton Park, Swansea, SA2 8PP, UK; i.sazonov@swansea.ac.uk.

even the only route to laminar–turbulent transition (e.g. Lin 1955; Chandrasekhar 1981; Drazin & Reid 1981). The relatively recent evidence that the so-called bypass scenarios of transition, where the linear modal instabilities are of little importance, are quite common (Jacobs & Durbin 2001), supported an alternative line of thought presented in clear and concise form in (e.g. Trefethen *et al.* 1993). Its essence lies in the observation that for a wide class of basic flows there exist perturbations of non-modal character which experience considerable transient growth within the framework of linear theory. This growth is expected to result in the triggering of nonlinear dynamics and secondary instabilities (Schmidt & Henningson 2001). We pursue a 'third way', conceptually very different from those outlined above. It is possible that in a flow without linear instabilities of significance or strong transient growth there are motions which are weakly decaying but nevertheless eventually become nonlinear and cause secondary instabilities, as will be shown in a later paper. In view of such a possibility the natural question regarding what happens to the arbitrary linearly stable perturbations in boundary layers, which seemed to be considered unworthy of attention as long as the perturbations are decaying, acquires a new importance.

The problem has been intensively studied in the context of the so-called spot dynamics by means of analytical, numerical and experimental approaches (see e.g. Smith, Dodia & Bowles 1994; Bowles & Smith 1995; Jacobs & Durbin 2001; and references therein). However, as was noted by Bowles & Smith (1995) *'there seem to be few if any linear or nonlinear studies of initial-value problems which are not restricted to narrow-band perturbations'*. Bowles & Smith (1995) addressed the challenge by considering a model problem where the boundary layer was approximated by a piecewise linear flow with one velocity break. The present work partly fills this gap by providing analytical treatment of the evolution of broadband perturbations for arbitrary continuous boundary layers.

The present paper is the second in a series on the quasi-modes (QM) introduced in the context of boundary layers in Shrira & Sazonov (2001) (hereinafter called Part 1). It is based upon specific results regarding the evolution of spatially monochromatic perturbations obtained in Part 1 and further develops the concept of quasi-modes. A quasi-mode is an approximate solution of the linear boundary-value problem composed of the Rayleigh equation and appropriate boundary conditions; the solution is described by the residue in the pole of the Green's function lying on a non-physical sheet of the complex plane (Landau pole). From the spectral viewpoint the quasi-mode represents a specific aggregate of normal modes of the continuous spectrum of the boundary-value problem mentioned. For harmonic perturbations of wavelength $2\pi/k$, long compared to the boundary layer thickness H, $kH \ll 1$, this aggregate, to the leading order in kH, behaves as if it were a single decaying mode of a discrete spectrum characterized by a specific dispersion relation. The quasi-modes are regular at the leading order in kH, have asymptotically small decay and represent an intermediate asymptotics over a large time interval $O((kH)^{-3})$. This means that with a good accuracy in this time interval the solution of the Cauchy problem for such long monochromatic perturbations can be described as the evolution of the corresponding quasi-mode, the discrepancy in terms of energy being $O((kH)^4)$ or smaller. In the present work we study the evolution of arbitrary broadband linear perturbations. While for each harmonic constituent of a perturbation the quasi-modes represent at best (and only for the long-wave components) their intermediate asymptotics, we show that large-time asymptotics of generic initial perturbations are described in terms of quasi-modes. The larger the times the better are the quasi-mode asymptotics.

There is a certain resemblance with the phenomenon known in geophysical fluid dynamics as 'geostrophic adjustment': if an arbitrary initial perturbation is considered within the framework of the full set of hydrodynamic equations then after a certain time the total motion will split into fast and slowly evolving constituents (Rossby 1937, 1938). The fast ones travel far away and, remarkably, their effect upon the slowly evolving constituents is negligible even with nonlinearity taken into account, while the evolution of the slow ones is governed by a much simpler closed system of equations (Reznik, Zeitlin & Ben Jelloul 2001). Thus, if we are concerned with the long-time field evolution it is sufficient to study only the subset of slow motions, provided we are able to find the long-time asymptotics of the transition problem, i.e. to project given initial conditions into the subset of slow motions. In our case, we also begin with arbitrary broadband initial conditions which after a certain transitional period produce long-wave perturbations, while the shorter high-frequency field components just die out. In the present paper we do not describe the entire transitional process; we find the asymptotics, which might be viewed as the *result of 'adjustment'*. Hereinafter we will use this term in this sense. To continue exploitation of the same analogy and to place it more clearly into the boundary layer context note that the so-called triple-deck asymptotic regime in boundary-layer theory (e.g. Smith 1982; Schmidt & Henningson 2001), being confined to long and slow motions, plays the role of the slow geostrophic subset; correspondingly, the derived asymptotics allow us to relate this regime to arbitrary broadband initial conditions.

The paper is organized as follows. In § 2 we begin with a standard mathematical formulation for two-dimensional motions in ideal incompressible fluid and outline the class of generic initial perturbations we consider. Following Part 1, in an arbitrary perturbation all constituent Fourier harmonics can be divided into three groups: the long-wave ones which obey the quasi-mode asymptotics from the start; those of even larger scale which initially are at the stage of initial transition and turn into quasi-modes at a certain later time; and shorter scales which never exhibit quasi-mode asymptotics. First, in § 3 we obtain rough estimates of the energy in each of these three constituent groups as a function of time. We show that for generic localized initial perturbations the quasi-mode constituent inevitably becomes dominant at large times. In the central § 4 the spatio-temporal structure of the large-time asymptotics is investigated in detail and a non-trivial field structure is revealed. The analytic results are verified by direct numerical simulation of the Cauchy problem for a few typical initial distributions. The concluding § 5 provides a brief discussion of some implications of the results. The present study is confined to small-amplitude inviscid two-dimensional perturbations; nonlinear, viscous and three-dimensional effects constitute the subject of the next parts of the series.

2. Initial-value problem for inviscid boundary-layer-type shear flows

2.1. *Statement of the problem*

We consider two-dimensional motions of ideal incompressible fluid of unit density. From the start we explicitly separate the perturbations and the basic flow. The latter is assumed to be steady and uniform with the velocity profile $\{\bar{U}(\bar{z}), 0, 0\}$, where $\bar{x}, \bar{y}, \bar{z}$ are the downstream, spanwise and vertical coordinates, respectively. Throughout the paper to distinguish dimensional variables from their non-dimensional counterparts we use an overbar for the dimensional ones. Although we will mostly use non-dimensional variables, some key results are presented in the dimensional form as well. We choose the Cartesian reference frame moving with the basic flow at infinity as

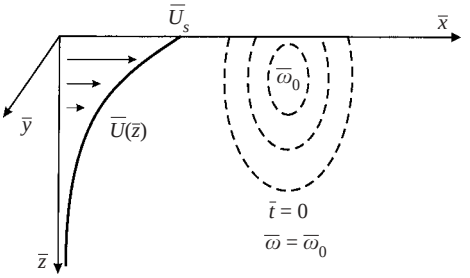

FIGURE 1. Sketch of geometry and notation showing initial perturbation ω_0 in a boundary-layer-type flow $U(z)$.

shown in figure 1, i.e. $\bar{U} \to 0$ as $\bar{z} \to \infty$ and $\bar{U} = \bar{U}_s > 0$ at the surface $\bar{z} = 0$. The frame convention we choose is typical of free-surface boundary layers; we use a model of wind-induced laminar boundary layer in water as the main example throughout the paper. Since the present study is confined to consideration of two-dimensional motions ($\partial_y \equiv 0$), it is convenient to introduce the perturbation stream function $\bar{\psi}$

$$\bar{u} = -\bar{\psi}_{\bar{z}}, \quad \bar{w} = \bar{\psi}_{\bar{x}} \quad (\text{let } \bar{\psi}(\bar{z} = 0) = 0), \tag{2.1}$$

where $\bar{u}$ and $\bar{w}$ are horizontal and vertical velocity perturbations. By taking the divergence of the Euler equations and making use of the continuity equation we reduce the governing equations to the form

$$(\partial_{\bar{t}} + \bar{U}\partial_{\bar{x}})\nabla^2\bar{\psi} - \bar{U}''\partial_{\bar{x}}\bar{\psi} = J\{\bar{\psi}, \nabla^2\bar{\psi}\}. \tag{2.2}$$

Here $\nabla^2 \equiv \partial_{\bar{x}}^2 + \partial_{\bar{z}}^2$, a prime means differentiation with respect to $\bar{z}$, although the subscripts $\bar{x}$ and $\bar{z}$ are also used below to denote the correspondent derivatives; J is the Jacobian of two functions. Introducing the vorticity of the perturbations $\bar{\omega}$ as

$$\bar{\omega} = \bar{w}_{\bar{x}} - \bar{u}_{\bar{z}} = \left(\partial_{\bar{x}}^2 + \partial_{\bar{z}}^2\right)\bar{\psi}, \tag{2.3}$$

we note that

$$J\{\bar{\psi}, \nabla^2\bar{\psi}\} = J\{\bar{\psi}, \bar{\omega}\} = \bar{\psi}_{\bar{z}}\bar{\omega}_{\bar{x}} - \bar{\psi}_{\bar{x}}\bar{\omega}_{\bar{z}} \equiv -(\bar{u}\bar{\omega}_{\bar{x}} + \bar{w}\bar{\omega}_{\bar{z}}). \tag{2.4}$$

We confine our present study to linear perturbations and thus neglect the Jacobian.

The boundary conditions are standard for this type of problem. We assume the 'no-flux' condition at the surface

$$\bar{w} \equiv \bar{\psi}_{\bar{x}} = 0 \quad \text{as } \bar{z} = 0. \tag{2.5}$$

The perturbations are also required to decay far from the surface:

$$\bar{\psi}, \bar{\omega}, \bar{u}, \bar{w} \to 0 \quad \text{as } \bar{z} \to \infty. \tag{2.6}$$

At the initial moment the velocity field satisfying (2.5)–(2.6) is assumed to be given:

$$\bar{\psi}(\bar{x}, \bar{z}, \bar{t} = 0) = \bar{\psi}_0(\bar{x}, \bar{z}) \tag{2.7}$$

By virtue of the chosen condition ($\bar{\psi}(\bar{z} = 0) = 0$) it is sufficient, and often more convenient, to present the above initial conditions in terms of the initial vorticity distribution

$$\bar{\omega}_0(\bar{x}, \bar{z}) \equiv \left(\partial_{\bar{x}}^2 + \partial_{\bar{z}}^2\right)\bar{\psi}_0. \tag{2.8}$$

The set of equations (2.2)–(2.8) prescribes the initial-value problem which is the subject of our study.

2.2. *Assumptions regarding the basic flow and initial disturbances*

We focus our attention on generic boundary-layer-type flows and generic perturbations. Below we formulate the assumptions ensuring that both the basic flow and initial perturbation do not contain pronounced small lengthscales in $\bar{z}$.

We introduce a characteristic flow thickness $\bar{H}$ as

$$\bar{H} = \frac{\bar{U}_s}{|\bar{U}'_s|}, \tag{2.9}$$

where $\bar{U}'_s \equiv \partial_{\bar{z}}\bar{U}(\bar{z}=0)$ is the gradient of the mean flow at the surface. Assume that the flow profile is smooth enough and does not contain characteristic scales smaller than $\bar{H}$, i.e.

$$\left|\bar{U}^{(n)}(z)\right| \lesssim \frac{\bar{U}_s}{\bar{H}^n}, \quad n = 1, 2, \ldots. \tag{2.10}$$

Assume the initial vorticity ω_0 to be localized in the layer $\bar{z} \lesssim H$ and decaying as $\bar{z}$ increases faster than $\bar{U}'$:

$$\frac{\bar{\omega}_0}{\bar{U}'} \to 0 \quad \text{as } \bar{z} \to \infty. \tag{2.11}$$

It is also assumed that the vertical scale of the initial distribution is of the same order as that of the basic flow and does not contain characteristic scales smaller than $\bar{H}$, i.e.

$$\left|\partial^n_{\bar{z}}\bar{\omega}_0\right| \lesssim \frac{|\bar{\omega}_0|}{\bar{H}^n}. \tag{2.12}$$

The initial perturbation is also expected to have a smooth spatial spectrum with respect to horizontal wavenumber without multiple peaks. We emphasize that we impose no restrictions on the dominant scale of the perturbations.

2.3. *Non-dimensional variables*

Finally, to conclude the mathematical formulation of the problem, we introduce non-dimensional variables using the scales $\bar{H}, |\bar{U}'_s|^{-1}, \bar{U}_s$ specified by the basic flow as follows:

$$x = \frac{\bar{x}}{\bar{H}}, \quad z = \frac{\bar{z}}{\bar{H}}, \quad t = \bar{t}|\bar{U}'_s|, \quad U = \frac{\bar{U}}{\bar{U}_s}, \quad u = \frac{\bar{u}}{\bar{U}_s}, \quad \ldots. \tag{2.13}$$

The use of these variables is equivalent to re-scaling the measured units in such a way that

$$U_s = 1, \quad U'_s = -1, \quad H = 1.$$

Equations (2.2)–(2.8) preserve their form in terms of these non-dimensional variables, i.e. remain the same with bars omitted.

3. Rough estimates

Having linearized the governing equation (2.2) we work within the framework of

$$(\partial_t + U\partial_x)\left(\partial_x^2 + \partial_z^2\right)\psi - U''\partial_x\psi = 0. \tag{3.1}$$

Applying the spatial Fourier transform

$$\hat{\psi}(t,k,z) = \int_{-\infty}^{+\infty} \psi(t,x,z)\mathrm{e}^{-\mathrm{i}kx}\mathrm{d}x, \quad \psi(t,x,z) = \frac{1}{2\pi}\int_{-\infty}^{+\infty} \hat{\psi}(t,k,z)\mathrm{e}^{\mathrm{i}kx}\mathrm{d}k, \tag{3.2}$$

we find that every spectral component $\hat{\psi}(t,k,z)$ satisfies the equation

$$(\partial_t + \mathrm{i}kU)\left(\partial_z^2 - k^2\right)\hat{\psi} - \mathrm{i}kU''\hat{\psi} = 0, \tag{3.3}$$

where $k = \bar{k}\bar{H}$ is a non-dimensional wavenumber. The properies of (3.3) are well-studied; in particular, the evolution of spatially harmonic components within its framework has been investigated thoroughly in Part 1. A summary of the relevant results is given below in § 3.1. The evolution of non-monochromatic perturbations proves to be qualitatively different. This section contains a preliminary analysis aimed at capturing its essential features.

3.1. *Spatially harmonic field: results*

The key point established in Part 1 is that the solution describing the evolution of each spatially harmonic component can be represented as a sum of two parts: a mode-like part $\hat{\psi}_{\mathrm{QM}}$, and a non-modal part decaying as t^{-2} when $t \to \infty$; the latter we call 'tail' and denote as $\hat{\psi}_{\mathrm{Tail}}$:

$$\hat{\psi} = \hat{\psi}_{\mathrm{QM}} + \hat{\psi}_{\mathrm{Tail}}, \tag{3.4a}$$

$$\hat{\psi}_{\mathrm{QM}}(x,z,t) = \hat{\psi}_{\mathrm{QM}}(z)\exp[\mathrm{i}k(x - c_p t)], \tag{3.4b}$$

$$\hat{\psi}_{\mathrm{Tail}}(x,z,t) \propto t^{-2}, \quad t \gg \max_z\{U''/(U')^2\}|k|^{-1}. \tag{3.4c}$$

Here c_p is an eigenvalue of the boundary value problem for $\psi(z;c)$:

$$\psi'' - k^2\psi - \frac{U''}{U-c}\psi = 0, \tag{3.5a}$$

$$\psi = 0 \quad \text{as } z = 0, \tag{3.5b}$$

$$\psi' + |k|\psi \to 0 \quad \text{as } z \to \infty. \tag{3.5c}$$

If $\operatorname{Im} c_p > 0$ solution of this problem gives a growing normal mode. If $\operatorname{Im} c_p < 0$, i.e. in the case we are primarily interested in, the problem (3.5*a–c*) must be solved on a complex z-plane on a contour passing around the point $z_c = U^{-1}(c)$ in accordance with Lin's rule (Lin 1955). Then the solution of this boundary-value problem gives the so-called quasi-mode (QM) (Briggs, Daugherty & Levy 1970; Part 1) which has a discontinuity in the critical layer. In the solution of the Cauchy problem this discontinuity is exactly compensated by the discontinuity in the non-modal part ψ_{Tail} having the opposite sign.

As was shown in Part 1, in the long-wave limit $|k| \equiv |\bar{k}\bar{H}| \ll 1$ the eigenvalue c_p can be approximated by:†

$$\operatorname{Re} c_p = 1 - |k| + O(k^2 \log k), \tag{3.6a}$$

$$\operatorname{Im} c_p = \begin{cases} \varkappa k^2 \operatorname{sgn} k + O(k^3 \log k), & U_s'' \neq 0 \\ \varkappa k^3 \operatorname{sgn} k + O(k^4 \log k), & U_s'' = 0. \end{cases} \tag{3.6b}$$

where $\varkappa$ is a constant specified by the basic flow at the surface:

$$\varkappa = \begin{cases} \pi U_s'' = \pi \bar{U}_s'' \bar{U}_s |\bar{U}_s'|^{-2}, & U_s'' \neq 0 \\ \pi U_s''' = \pi \bar{U}_s''' \bar{U}_s^2 |\bar{U}_s'|^{-3}, & U_s'' = 0. \end{cases} \tag{3.7}$$

† In Part 1 all formulae are given for positive k. Here they are generalized to be valid for negative k as well, which is essential for our further consideration.

In this paper we are primarily concerned with non-degenerate basic flows for which $U_s'' \neq 0$, although the case $U_s'' \neq 0$ is not uncommon. The Blasius boundary layer is even more degenerate: $U_s'' = 0$ and $U_s''' = 0$. It can be treated similarly.

For convenience, it is also worthwhile to present the formulae for the leading terms of real and imaginary parts of the eigenvalue c_p in dimensional form:

$$\operatorname{Re} \bar{c}_p \simeq \bar{U}_s + \frac{\bar{U}_s^2}{\bar{U}_s'} |\bar{k}|, \quad \operatorname{Im} \bar{c}_p \simeq \begin{cases} \pi \dfrac{\bar{U}_s'' \bar{U}_s^4}{\bar{U}_s'^4} \bar{k}^2 \operatorname{sgn} \bar{k}, & \bar{U}_s'' \neq 0 \\ \pi \dfrac{\bar{U}_s''' \bar{U}_s^6}{\bar{U}_s'^6} \bar{k}^3 \operatorname{sgn} \bar{k}, & \bar{U}_s'' = 0. \end{cases}$$

For large and intermediate $|k|$ the dependence $c_p(k)$ can be found numerically (see Part 1); $c_p(k)$ has finite negative imaginary part for all examples of particular boundary-layer-type flows studied in Part 1, and this will be assumed to be the case here too.

For the long-wave perturbations (where $c_i \equiv \operatorname{Im} c_p$ is small) the quasi-mode dominates over a wide time interval $t_1 < t < t_2$ where

$$t_1 \sim |k|^{-1}, \qquad t_2 \sim \begin{cases} |k|^{-3} \log(1/|k|), & U_s'' \neq 0 \\ |k|^{-4} \log(1/|k|), & U_s'' = 0. \end{cases} \tag{3.8}$$

Here the interval of dominance was defined using the energy criterion. If the criterion were based upon dominance in terms of different field components, we would arrive at the same estimate for t_2 if we choose ψ or w. If we choose a criterion based upon horizontal velocity u, then t_2 would be $1/|k|$ times smaller. See Part 1 for details.

At small times, $t \lesssim t_1$, an *initial transition* takes place: initial perturbations might grow or decay, but essentially the mode-like and non-modal parts remain of the same order as the initial perturbation.

For large times, $t \gtrsim t_2$, the non-modal part inevitably dominates and the total disturbance decays as t^{-2}.

For the intermediate and short waves ($|k| \gtrsim 1$) the perturbation field does not exhibit any intermediate QM-type asymptotics; in this case the initial transition ($t \ll |k|^{-1}$) is directly followed by the t^{-2} decay ($t \gg |k|^{-1}$) although some traces of QM asymptotics can be found for $|k|$ up to unity (see Part 1).

It is worth noting that, although the numerics of Part 1 show that $c_i \equiv \operatorname{Im} c_p$ tends to zero when $|k| \to \infty$, nevertheless the quasi-mode can be disregarded for sufficiently large $|k|$. In this case the quasi-mode does not contribute to the solution of the initial value problem since the pole associated with the quasi-mode passes beneath the vertical cut drawn from the branch point $\bar{c} = \bar{U}_s$ (see figure 6 in Part 1 for details).

3.2. *Generic non-monochromatic perturbations: QM domination*

Based on the acquired understanding of spatially monochromatic perturbations summarized above, now we are in position to consider, at first qualitatively, the evolution of an arbitrary broadband perturbation at comparatively large times $t \gg 1$. By that time all short ($|k| \gg 1$) and intermediate ($|k| \sim 1$) harmonic components are at the stage of the t^{-2} decay. The long-wave components ($|k| \ll 1$) can be split into two groups:

(i) For all times t there always exist the longest wave components which still are at the stage of initial transition ψ_{Ini}. We estimate the upper boundary for those

components from (3.8):

$$|k| < k_1(t) \sim t^{-1}. \tag{3.9}$$

(ii) When $|k| > k_1$ we represent the perturbation as a sum of the modal (3.4*b*) part and the tail (3.4*c*). The tail dominates if (see (3.8))

$$|k| > k_2(t) \sim t^{-1/3} \gg k_1(t) \tag{3.10}$$

($k_2 \sim t^{-1/4}$ if $U_s'' = 0$, but $U_s''' \neq 0$). The QM asymptotics dominates when $k \in [k_1, k_2]$.

Thus we can represent the total solution as a sum of these parts:

$$\psi \simeq \psi_{\text{Ini}} + (\psi_{\text{QM}} + \psi_{\text{Tail}}), \tag{3.11a}$$

$$\psi_{\text{Ini}} \simeq \frac{1}{2\pi} \int_{-k_1}^{k_1} \hat{\psi}(k, z, t) \mathrm{e}^{\mathrm{i}kx}\, \mathrm{d}k, \tag{3.11b}$$

$$\psi_{\text{QM}} \simeq \frac{1}{2\pi} \left\{ \int_{-\infty}^{-k_1} + \int_{k_1}^{\infty} \right\} \hat{\psi}_{\text{QM}}(z, k) \mathrm{e}^{\mathrm{i}kx - \mathrm{i}kc_p t}\, \mathrm{d}k, \tag{3.11c}$$

$$\psi_{\text{Tail}} \simeq \frac{1}{2\pi} \left\{ \int_{-\infty}^{-k_1} + \int_{k_1}^{\infty} \right\} \hat{\psi}_{\text{Tail}}(z, k, t) \mathrm{e}^{\mathrm{i}kx}\, \mathrm{d}k. \tag{3.11d}$$

3.2.1. *Preliminary definitions*

The total energy of a perturbation $E(t)$ can be represented in two forms:

$$\int_{-\infty}^{+\infty} \mathrm{d}x \int_0^{\infty} \mathrm{d}z\, \frac{u^2 + w^2}{2} = E(t) = \frac{1}{2\pi} \int_{-\infty}^{+\infty} \mathrm{d}k \int_0^{\infty} \mathrm{d}z\, \frac{|\hat{u}|^2 + |\hat{w}|^2}{2}. \tag{3.12}$$

This follows from the fact that for every z by virtue of the Parseval's identity

$$\int_{-\infty}^{+\infty} \mathrm{d}x\, \frac{u^2 + w^2}{2} = \frac{1}{2\pi} \int_{-\infty}^{+\infty} \mathrm{d}k\, \frac{|\hat{u}|^2 + |\hat{w}|^2}{2},$$

and after integration with respect to z and change of the order of integration we obtain (3.12).

We introduce spatial and spectral energy densities:

$$\rho(x, t) = \int_0^{\infty} \mathrm{d}z\, \frac{u^2 + w^2}{2}, \qquad \hat{\rho}(k, t) = \frac{1}{2\pi} \int_0^{\infty} \mathrm{d}z\, \frac{|\hat{u}|^2 + |\hat{w}|^2}{2}.$$

Then

$$E(t) = \int_{-\infty}^{+\infty} \mathrm{d}x\, \rho(x, t) = \int_{-\infty}^{+\infty} \mathrm{d}k\, \hat{\rho}(k, t), \tag{3.13}$$

i.e. the instantaneous energy of the perturbation $E(t)$ can be represented as a sum of energies of the all wave components. Since $\hat{\rho}(k, t)$ is an even function with respect to k,

$$E(t) = 2 \int_0^{+\infty} \hat{\rho}(k, t)\, \mathrm{d}k.$$

The evolution of $\hat{\rho}(k, t)$ has been studied in Part 1, where it is denoted as $E(t)$, which is $2\pi\hat{\rho}(k, t)$ in the present notation.

3.2.2. *Estimations of the constituents*

We split integral (3.13) into three parts in the same manner as in (3.11):

$$E(t) = E_{\text{Ini}} + (E_{\text{QM}} + E_{\text{Tail}}) \simeq 2 \int_0^{k_1} \hat{\rho}_{\text{Ini}}\, \mathrm{d}k + \left(2 \int_{k_1}^{\infty} \hat{\rho}_{\text{QM}}\, \mathrm{d}k + 2 \int_{k_1}^{\infty} \hat{\rho}_{\text{Tail}}\, \mathrm{d}k \right). \tag{3.14}$$

Part	Decay of $\hat{\rho}(k,t)$ with respect to t
$\hat{\rho}_{\mathrm{Ini}}(\lvert k\rvert < k_1)$	Remains of order of $\hat{\rho}_{00}$
$\hat{\rho}_{\mathrm{QM}}(k_1 < \lvert k\rvert < k_2)$	$\exp(2c_i t) \sim \exp(-2\varkappa k^3 t)(\sim\exp(-2\varkappa k^4 t)$, the Blasius flow)
$\hat{\rho}_{\mathrm{Tail}}(\lvert k\rvert > k_1)$	$(kt)^{-2}$

TABLE 1. Decay law for each constituent of $\hat{\rho}(k,t)$ based on results in Part 1.

Note that we can split the energy densities for the tail and modal-part:

$$\begin{aligned} E_{\mathrm{QM}} + E_{\mathrm{Tail}} &= \int_{k_1}^{\infty} \mathrm{d}z\, \frac{|\hat{u}_{\mathrm{QM}} + \hat{u}_{\mathrm{Tail}}|^2 + |\hat{w}_{\mathrm{QM}} + \hat{w}_{\mathrm{Tail}}|^2}{2} \\ &= \int_{k_1}^{\infty} \mathrm{d}z\, \frac{|\hat{u}_{\mathrm{QM}}|^2 + |\hat{w}_{\mathrm{QM}}|^2}{2} + \int_{k_1}^{\infty} \mathrm{d}z\, \frac{|\hat{u}_{\mathrm{Tail}}|^2 + |\hat{w}_{\mathrm{Tail}}|^2}{2} \\ &\quad + \int_{k_1}^{\infty} \mathrm{d}z\, (|\hat{u}_{\mathrm{QM}}\hat{u}_{\mathrm{Tail}}| + |\hat{w}\hat{w}_{\mathrm{Tail}}|) \end{aligned}$$

The last integral is much smaller than either of the first two. This is due to the oscillatory behaviour in z of the tail: $\hat{u}_{\mathrm{Tail}}, \hat{w}_{\mathrm{Tail}} \propto \mathrm{e}^{-\mathrm{i}kU(z)t}$, whereas $\hat{u}_{\mathrm{QM}}$ and $\hat{w}_{\mathrm{QM}}$ have a characteristic lengthscale of the order $\bar{H}$ (see Part 1 for details). Thus,

$$E_{\mathrm{QM}} + E_{\mathrm{Tail}} \simeq 2\int_{k_1}^{\infty} \hat{\rho}_{\mathrm{QM}}\, \mathrm{d}k + 2\int_{k_1}^{\infty} \hat{\rho}_{\mathrm{Tail}}\, \mathrm{d}k. \tag{3.15}$$

Now we estimate the contribution of each part in (3.14). We consider the initial perturbations whose spectrum $\hat{\rho}(k,0)$ is a smooth function without multiple peaks. First we consider the generic situation when the spectrum tends to a non-zero constant $\hat{\rho}(k,0) \to \hat{\rho}_{00} > 0$ as $k \to 0$. Then the spectrum corresponds to a single monopole vortex near the surface. The evolution of more general classes of perturbations will be dealt with below.

At this stage within the framework of linear analysis we are free to choose the normalization of the perturbation amplitude, and to simplify the formulae we assume for the time being that the constant $\hat{\rho}_{00}$ is of order of unity.

Short-wave components decay faster than long-wave ones; therefore for sufficiently large time t the perturbation energy is determined by the long-wave components such that $\hat{\rho}(k,0) \sim \hat{\rho}_{00} \sim 1$.

The decay laws for every constituent based on the results of Part 1 are summarized in table 1.

(i) E_{Ini}: We begin with the longest, $k < k_1$, components which are still in the stage of the initial transition. Taking into account (3.9) it is easy to find

$$E_{\mathrm{Ini}}(t) \approx 2\int_0^{k_1} \hat{\rho}(k,t)\, \mathrm{d}k \sim 2\hat{\rho}_{00}\int_0^{t^{-1}} \mathrm{d}k \sim t^{-1}. \tag{3.16}$$

(ii) E_{QM}: The contribution of the QM-part is estimated as follows:

$$\begin{aligned} E_{\mathrm{QM}}(t) \approx 2\int_{k_1}^{k_2} \hat{\rho}_{\mathrm{QM}}(k,0)\, \exp(2c_i(k)t)\, \mathrm{d}k &\sim 2\int_{t^{-1}}^{t^{-1/3}} \exp(-2\varkappa k^3 t)\, \mathrm{d}k \\ &\sim \int_{t^{-1}}^{\infty} \exp(-2\varkappa k^3 t)\, \mathrm{d}k. \end{aligned}$$

Substitution $s = 2\varkappa k^3 t$ yields

$$E_{\mathrm{QM}}(t) \sim \frac{1}{\left(2\varkappa t^{1/3}\right)} \int_{2\varkappa t^{-2}}^{\infty} \frac{\mathrm{e}^{-s}}{s^{2/3}}\,\mathrm{d}s \sim \frac{1}{(2\varkappa t)^{1/3}} \left[\int_0^{\infty} \frac{\mathrm{e}^{-s}}{s^{2/3}}\,\mathrm{d}s + O\left(t^{-2/3}\right) \right] \sim t^{-1/3} \quad (3.17)$$

as $\int_0^{\infty} s^{-2/3}\mathrm{e}^{-s}\,\mathrm{d}s = \Gamma(1/3) \approx 2.68 \sim 1$ (For the $U_s'' = 0$ and $U_s''' \neq 0$ case we would have $E_{\mathrm{QM}}(t) \sim t^{-1/4}$).

(iii) E_{Tail}: The contribution of the tail is

$$E_{\mathrm{Tail}}(t) \approx \int_{k_1}^{\infty} \hat{\rho}_{\mathrm{Tail}}(k, t)\,\mathrm{d}k \sim \hat{\rho}_{00} \int_{t^{-1}}^{\infty} k^{-2} t^{-2}\,\mathrm{d}k \sim t^{-1}. \quad (3.18)$$

Note that all contributions to E_{Tail} and E_{QM} are taken into account, including the spectral intervals where the corresponding perturbation constituents are not dominating.

3.2.3. *Discussion*

The principal conclusion of profound importance which immediately follows from the estimations above is that for sufficiently large times the QM contribution necessarily dominates. Although for every harmonic component the mode-like part represents intermediate asymptotics only, nevertheless it is the true asymptotics for a generic initial perturbation with broadband initial spatial spectrum. At first sight the components which are in the stage of initial transition should dominate, as they do not decay. However, their contribution rapidly diminishes since the corresponding spectral interval narrows as t^{-1}. Thus for sufficiently large time we obtain

$$\frac{E_{\mathrm{QM}}}{E_{\text{non-modal}}} = \frac{E_{\mathrm{QE}}}{E - E_{\mathrm{QE}}} \sim t^{2/3}, \quad t \to \infty \quad (3.19)$$

($\sim t^{3/4}$ for the case $U_s'' = 0$, $U_s''' \neq 0$).

This fundamental assertion, formulated in terms of energy, also remains valid if we are primarily interested in w or ψ components of the perturbation. Qualitatively similar behaviour can be obtained in terms of the horizontal velocity u as well (see below).

3.3. *Behaviour of non-generic perturbations*

Apart from the generic initial perturbations studied above, there are also situations of interest where an initial perturbation has a smooth initial spectrum of ψ decaying as k^n as $k \to 0$. Then the spectral energy density behaves as k^{2n} near zero. For natural n this spectrum corresponds to a vortex multipole of order n. If the initial perturbation is not localized but is a noise-like signal, its spectrum can have fractional n. As our speculations in this Section hold for such perturbations, we incorporate them in our analysis as well.

For such perturbations, proceeding similarly we find the following estimates:

$$E_{\mathrm{Ini}}(t) \sim t^{-(2n+1)}, \quad (3.20a)$$

$$E_{\mathrm{QM}}(t) \sim t^{-(2n+1)/3}, \quad (3.20b)$$

$$E_{\mathrm{Tail}}(t) \sim \begin{cases} t^{-(2n+1)}, & n < 1/2 \\ t^{-2}, & n \geqslant 1/2. \end{cases} \quad (3.20c)$$

The evaluation of E_{Tail} needs some explanation. If $n < 1/2$ the integral $\int_{k_1}^{\infty} k^{2n-2}\,\mathrm{d}k$ converges and the main contribution to E_{Tail} is due to the vicinity of k_1. If $n > 1/2$ the

integral $\int_{k_1}^{\infty} k^{-2+n}\,\mathrm{d}k$ diverges at infinity whereas the integral $\int_{k_1}^{\infty} \hat{\rho}(k,t)k^{-2}\,\mathrm{d}k$ converges (as $\int_{k_1}^{\infty} \hat{\rho}(k,t)\,\mathrm{d}k$ converges). This means that the short-wave components should be taken into account, for which the spectrum ceases to be k^{2n}. We can put

$$E_{\mathrm{Tail}} = t^{-2}\int_{k_1}^{\infty} \hat{\rho}(k,0)k^{-2}\,\mathrm{d}k = t^{-2}\int_{k_1}^{k_*} \hat{\rho}(k,0)k^{-2}\,\mathrm{d}k + t^{-2}\int_{k_*}^{\infty} \hat{\rho}(k,0)k^{-2}\,\mathrm{d}k,$$

where $k_* \ll 1$ and does not depend on t; then $\hat{\rho}(k_*,0) \approx k_*^n$. Thus

$$E_{\mathrm{Tail}} = t^{-2}\int_{k_1}^{k_*} k^{2n-2}\,\mathrm{d}k + t^{-2}A,$$

where $A = \int_{k_*}^{\infty} \hat{\rho}(k,0)k^{-2}\,\mathrm{d}k$ does not depend on t. The first integral can be estimated roughly as

$$t^{-2}\int_{k_1}^{k_*} k^{2n-2}\,\mathrm{d}k \sim \begin{cases} t^{-2n-1}, & n < 1/2 \\ t^{-2}k_*^{n-1}, & n > 1/2. \end{cases}$$

The proportion of the modal part obeys the relation

$$\frac{E_{\mathrm{QM}}}{E_{\text{non-modal}}} \sim t^{\nu}, \quad \nu = \begin{cases} \frac{2}{3} + \frac{4}{3}n, & n < 1/2 \\ \frac{5}{3} - \frac{2}{3}n, & n > 1/2, \end{cases} \tag{3.21}$$

which gives the following values of the time exponent ν for different values of n:

The spectrum exponent, n	0	1/2	1	3/2	2	5/2	3
The time exponent, ν	2/3	4/3	1	2/3	1/3	0	−1/3

It is worth mentioning that at first sight it seems easier to split interval $[k_1, \infty)$ into two: $[k_1, k_2]$ and $[k_2, \infty)$ where the QM part and the tail dominate, respectively, and after integration over these intervals we obtain estimations for the QM part and the tail. In fact, if we integrate the QM part within the limits $[k_1, k_2]$ we arrive at the same estimate. As for the tail, we have to include the components from the interval $[k_1, k_2]$ despite the fact that they are much smaller there compared to the QM part. Nevertheless, they are much greater than the shorter-wave components, and if we exclude the interval $[k_1, k_2]$ in the integration we noticeably underestimate energy of the tail for $n < 1/2$.

3.4. *The rough estimates: conclusion and discussion*

The conclusion from the above rough estimates is that the QM part dominates (in terms of energy) if $n < 5/2$: that is for the most common vortex monopoles ($n = 0$), as well as for vortex dipoles ($n = 1$) and quadrupoles ($n = 2$) the quasi-mode is the true asymptotics.

For higher-order vortex multipoles the formulae suggest otherwise. The answer, however, is not obvious, and a more elaborate analysis is needed. We stress that we estimated *global* energy in *the whole flow domain*. As we see below, for the initially localized perturbation, different parts of the evolving perturbation dominate in different regions of the flow. Say, the tail component is advected by $\bar{U}(\bar{z})$ and, therefore, is expected to be concentrated along the line $\bar{x} = \bar{U}(\bar{z})\,\bar{t}$; we would expect the 'initial transition' part of the field to be roughly uniformly distributed in z and x

in all the domain occupied by perturbation, while the QM component is concentrated in the vicinity of the front $\bar{x} = \bar{U}_s \bar{t}$. Hence we can expect the dominance of the QM part to be even more pronounced and to hold for a wider range situations if we consider its energy (or other field components) *locally*. The time–space evolution of the local structure of the field is the subject of the next section.

4. Large-time asymptotics

Having established that within the framework of linear theory the QM part dominates the perturbation field at large times in most conceivable cases of interest, now consider the evolution of an arbitrary broadband perturbation in more detail. We focus on evaluation of the QM component starting with integral presentation (3.11). For the sake of brevity we confine our attention to the generic flows with $U_s'' \neq 0$. The case $U'' = 0$ can be considered in a similar way.

For any kth wave component we can represent $\hat{\psi}_{\mathrm{QM}}$ as a product of an eigenfunction $\tilde{\psi}_{\mathrm{QM}}(z;k)$ describing the vertical structure of the quasi-mode, and its initial complex amplitude $\hat{a}(k)$. Then we can re-write (3.11) as

$$\psi_{\mathrm{QM}}(x, z, t) = \frac{1}{2\pi} \int_{-\infty}^{+\infty} \tilde{\psi}_{\mathrm{QM}}(z;k)\, \hat{a}(k)\, \mathrm{e}^{\mathrm{i}k(x - c_p t)}\, \mathrm{d}k. \tag{4.1}$$

Notice that we include the longest wave interval $[-k_1, k_1]$ in the integral (4.1) to simplify the formulae and to avoid artifacts caused by an abrupt cutoff of the spectrum. As we showed in § 3 the long-wave contribution due to this expansion of the integration domain is negligibly small in the region of interest.

The following observation enables us to simplify dramatically consideration of the basic integral (4.1). Since the quasi-mode phase velocity $c_p(k)$ has finite negative imaginary part for all but the longest k: $c_i(k) \to 0$ as $k \to 0$, only long-wave components 'survive' and contribute to the large-time asymptotics. Therefore, if we take whichever formula for $c_i(k)$ that provides a sufficient damping for large and intermediate k and has correct asymptotic behaviour for small k, we obtain the asymptotically correct result (i.e. when $t \to \infty$). Similarly we can take any convenient formulae for $\tilde{\psi}_{\mathrm{QM}}(z;k), \hat{a}(k), c_r(k)$ if they have the right long-wave asymptotics and do not have singularities at other wavelengths. These rather intuitive speculations will be supported by the rigorous results below. Now we can formulate the strategy we adopt in this section.

First, in § 4.1 we present the main terms in the long-wave expansion for the phase velocity and the mode structure which will be used throughout the section. Being interested in the asymptotic behaviour of the localized perturbations characterized by initial horizontal scale $\bar{L}$, we distinguish two qualitatively different cases. We begin with the more general case: the initial disturbance is broadband, i.e. is not initially a long-wave one, which implies $\bar{L} \geqslant O(\bar{H})$. In the course of its evolution such a perturbation inevitably turns into a long-wave one. Analysis of its large-time asymptotics is the subject of § 4.2. The important particular case of the *initially long-wave* perturbations ($\bar{L} \gg \bar{H}$) is considered in § 4.3. The evolution of the vorticity field is qualitatively different from that of the velocity components and therefore requires a special consideration. The issue is dealt with in § 4.4. The range of situations where the QM asymptotics works, found in § 3 on the basis of rough estimates, is refined in § 4.5. A comparison of the derived analytic formulae with a direct numerical simulation is carried out in § 4.6.

4.1. *Long-wave approximation for the quasi-mode*

First we employ the main-terms expansion in k for the phase velocity derived in Part 1:

$$c_p \simeq 1 - |k| - \mathrm{i}\varkappa k|k|. \tag{4.2}$$

Although this formula somewhat overestimates the damping for intermediate k (see Part 1, § 5.1), by virtue of the observation made above this does not affect the large-time asymptotics of integral (4.1).

The simplified formulae of the long-wave expansion for the vertical structure of the quasi-mode yield the main term of the expansions for different field components (see Part 1 and also Shrira 1989):

$$\tilde{\psi}_{\mathrm{QM}} = U - 1, \qquad \tilde{u}_{\mathrm{QM}} = -U', \qquad \tilde{w}_{\mathrm{QM}} = \mathrm{i}k\,(U-1), \qquad \tilde{\omega}_{\mathrm{QM}} = U''. \tag{4.3}$$

Note that since these eigenfunctions are normalized to keep $\tilde{u}_{\mathrm{QM}}(z=0) = 1$, then in the long-wave approximation the amplitude $\hat{a}(k)$ is simply equal to kth wave component of the horizontal velocity of the initial perturbation at the surface $\hat{u}_0(k, z=0)$. Thus

$$a(k) \cong \hat{u}_0(k, 0)\ [1 + O(k)]\,. \tag{4.4}$$

Substituting (4.3) and (4.4) into (4.1) we obtain

$$\hat{\psi}_{\mathrm{QM}} \simeq (U-1)\,\frac{1}{2\pi}\int_{-\infty}^{+\infty} \hat{u}_0(k, 0)\,\mathrm{e}^{\mathrm{i}k(x-c_p t)}\,[1 + O(k)]\,\mathrm{d}k, \tag{4.5}$$

where c_p is given by long-wave approximation (4.2). The description of the evolution is thus reduced to an analysis of (4.5), which is studied below in detail for different cases.

4.2. *Broadband perturbations*

Consider the asymptotic behaviour of initially localized broadband perturbations of initial horizontal scale $\bar{L} \lesssim \bar{H}$. Its initial spacial spectrum is assumed to be smooth to allow Taylor's expansion in k to any order.

4.2.1. *Integrals I_n*

Expand the initial spectrum $\hat{u}_0(k, 0)$ in (4.5) into the Taylor's series

$$\hat{u}_0(k, 0) = \sum_{n=0}^{\infty} \alpha_n (\mathrm{i}k)^n, \quad \alpha_n = \frac{1}{n!}\,\frac{\partial^n}{\partial(\mathrm{i}k)^n}\hat{u}_0(k, 0)\bigg|_{k=0}. \tag{4.6}$$

Since

$$\frac{\partial^n}{\partial(\mathrm{i}k)^n}\,\mathrm{e}^{\mathrm{i}kx}\bigg|_{k=0} = x^n, \quad \alpha_n = \frac{1}{n!}\int_{-\infty}^{+\infty} x^n u_0(x, 0)\,\mathrm{d}x,$$

we can express ψ_{QM} in terms of integrals $I_n(x, t)$ as follows:

$$\psi_{\mathrm{QM}}(x, z, t) \simeq [U(z) - 1] \sum_{n=0}^{\infty} \alpha_n I_n(x, t), \tag{4.7a}$$

$$I_n(x, t) = \frac{1}{2\pi}\int_{-\infty}^{+\infty} (\mathrm{i}k)^n \mathrm{e}^{\mathrm{i}k(x-c_p t)}\,\mathrm{d}k. \tag{4.7b}$$

Similar formulae can be also obtained for the velocity and vorticity components:

$$u_{\mathrm{QM}} \simeq -U' \sum_{n=0}^{\infty} \alpha_n I_n, \quad w_{\mathrm{QM}} \simeq (U-1) \sum_{n=0}^{\infty} \alpha_n I_{n+1}, \quad \omega_{\mathrm{QM}} \simeq U'' \sum_{n=0}^{\infty} \alpha_n I_n. \tag{4.8}$$

Thus, the problem of the evolution, already reduced to the analysis of integral (4.5) specific for each initial perturbation, has been further reduced to study of integrals I_n which do not depend on the initial perturbation. Moreover, for integer n, it is sufficient to consider just I_0 as all other integrals can be obtained by simple differentiation with respect to x:

$$I_n = \partial_x^n I_0. \tag{4.9}$$

From the asymptotic estimate

$$I_n \sim \frac{I_{n-1}}{t^{1/2}} \tag{4.10}$$

which we show below it follows that in the large-time asymptotics the term with the lowest n with non-zero α_n prevails, which further dramatically simplifies the description of the perturbation evolution. We denote as $n_{\min}$ the minimal n for which $\alpha_n \neq 0$.

The specificity of the initial distribution manifests itself primarily in the value of $n_{\min}$ for a given perturbation. For example, to describe the large-time evolution to the leading order, we need, in the case of a monopole, just I_0 for ψ and u and I_1 for w; to describe a dipole I_1 and I_2 are needed, respectively.

4.2.2. *Preliminary analysis of I_0 based on a dispersion relation*

A rough picture of the behaviour of I_0 can be reconstructed by means of a simple analysis based on the explicit quasi-mode dispersion relation (4.2). From (4.2) it is easy to find the quasi-mode group velocity C_g(we give its dimensional form $\bar{C}_g$ as well):

$$C_g = \frac{\mathrm{d}}{\mathrm{d}k} k \mathrm{Re} c_p = 1 - 2|k|, \qquad \bar{C}_g = \bar{U}_s - 2\frac{\bar{U}_s^2}{|\bar{U}_s'|}|\bar{k}|.$$

Since the maximum of the group velocity $\bar{U}_s$ is attained at $k = 0$, we should expect the perturbation front to be at $\bar{x} = \bar{U}_s \bar{t}$ ($x = t$). The greater the wavenumber of a harmonic constituent of the perturbation is, the lower is its celerity determined by the real part of the phase velocity and the greater is its damping, which is determined by its imaginary part. For large times the perturbation in the vicinity of a point moving with a velocity $v = x/t < 1$ (and $1 - v \ll 1$) is constituted by the components with the wavenumbers

$$|k(v)| \cong \frac{\Delta v}{2},$$

where $\Delta v = 1 - v$ ($\Delta \bar{v} = \bar{U}_s - \bar{x}/\bar{t}$) is velocity relative to the front in the opposite direction to the flow.

Without the Landau damping the dispersion would be the same as in the linearized Benjamin–Ono equation, while the local amplitude would decay uniformly for all k. The Landau damping described by the factor

$$\exp(-\varkappa |k|^3 t) = \exp\left(-\varkappa \frac{(\Delta v)^3}{8} t\right) \tag{4.11}$$

causes faster decay of higher-wavenumber harmonics. Due to the cube in the exponent, the decay becomes very abrupt when Δv exceeds an $O(t^{-1/3})$ value whereas harmonics with $k(v)$ such that $\Delta v < O(t^{-1/3})$ remain almost unaffected.

Thus, we can expect only a long-wave oscillating perturbation to survive and to be confined to an expanding zone (the QM-zone) specified by the inequalities

$$0 < \Delta v < O\left(t^{-1/3}\right) \Leftrightarrow t - O\left(t^{2/3}\right) < x < t.$$

The study of this asymptotic regime is carried out below.

4.2.3. *Analytical study of I_0 for large t*

Now we elaborate the above conclusion based on a semi-qualitative consideration by direct asymptotic analysis of integral (4.7). Substituting (4.2) into (4.7) and setting $n = 0$ we arrive at the integral

$$I_0 = \frac{1}{2\pi}\int_{-\infty}^{+\infty} \exp\{\mathrm{i}k(x-t) + \mathrm{i}k\,|k|\,t - \varkappa k^2\,|k|\,t\}\,\mathrm{d}k. \tag{4.12}$$

Splitting the integral into two: for positive and negative k, and then changing $k \to -k$ in the integral for negative k we obtain a more convenient integral:

$$I_0 = \frac{1}{2\pi}\int_{0}^{+\infty} \exp\{\mathrm{i}k(x-t) + \mathrm{i}k^2 t - \varkappa k^3 t\}\,\mathrm{d}k + \text{c.c.} \tag{4.13}$$

For our asymptotic study it is convenient to introduce a stretched coordinate X with the origin at the front $x = t$ and a correspondingly scaled wavenumber K as follows:

$$X = \frac{x-t}{t^{1/2}} = -\Delta v\, t^{1/2}, \quad K = kt^{1/2}. \tag{4.14}$$

Then we re-write integral I_0 in the form

$$I_0 = \frac{1}{2\pi t^{1/2}}\int_{0}^{+\infty} \exp\left\{\mathrm{i}KX + \mathrm{i}K^2 - \varkappa K^3 t^{-1/2}\right\}\mathrm{d}K + \text{c.c.} \tag{4.15}$$

Notice that if we neglect the Landau damping, assuming $\varkappa = 0$ (recall that $\varkappa$ is proportional to U''), then integral (4.15) can be taken explicitly, (we present the formula for its first derivative $I_1^{\varkappa=0}$ as well):

$$I_0^{\varkappa=0} = \frac{1}{\sqrt{2\pi t}}\,g\left(\frac{X}{\sqrt{2\pi}}\right), \qquad I_1^{\varkappa=0} = \partial_x I_0^{\varkappa=0} = \frac{1}{2\pi t}\left(\sqrt{\frac{\pi}{2}}X\,f\left(\frac{X}{\sqrt{2\pi}}\right) - 1\right),$$

where $g(Z)$ and $f(Z)$ are the auxiliary Fresnel's functions (see Abramowitz & Stegun 1965, 7.3.5, 7.3.6):

$$g(Z) = \left[\tfrac{1}{2} - C(Z)\right]\cos\frac{\pi Z^2}{2} + \left[\tfrac{1}{2} - S(z)\right]\sin\frac{\pi Z^2}{2},$$

$$f(Z) = \left[\tfrac{1}{2} - S(Z)\right]\cos\frac{\pi Z^2}{2} - \left[\tfrac{1}{2} - C(z)\right]\sin\frac{\pi Z^2}{2},$$

$$C(Z) = \int_0^Z \cos\frac{\pi z^2}{2}\,\mathrm{d}z, \quad S(Z) = \int_0^Z \sin\frac{\pi z^2}{2}\,\mathrm{d}z.$$

Functions $I_0^{\varkappa=0}$ and $I_1^{\varkappa=0}$ are plotted in figure 2. Their main features worth noting are that the period of oscillations increases as $(-X)$ grows, the maxima are of the same height for I_0 and grow with $(-X)$ for I_1. Note that the scaled coordinate X is a self-similar one for $I_n^{\varkappa=0}$. Function $I_0^{\varkappa=0}$ has a transparent interpretation: it is the Green's function for the linearized Benjamin–Ono equation.

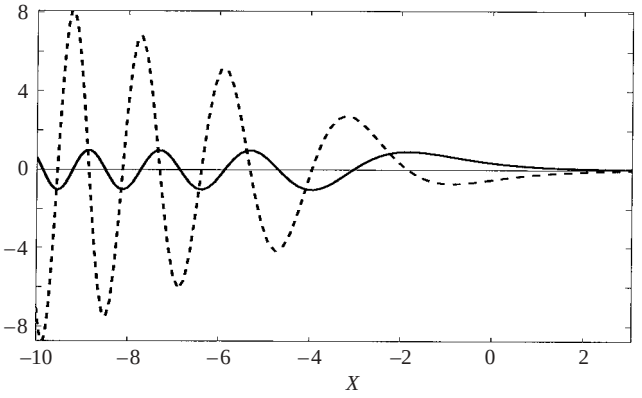

FIGURE 2. $(\pi t)^{1/2} I_0^{\varkappa=0}$ (solid) and $(\pi t) I_1^{\varkappa=0}$ (dotted) versus self-similar variable X.

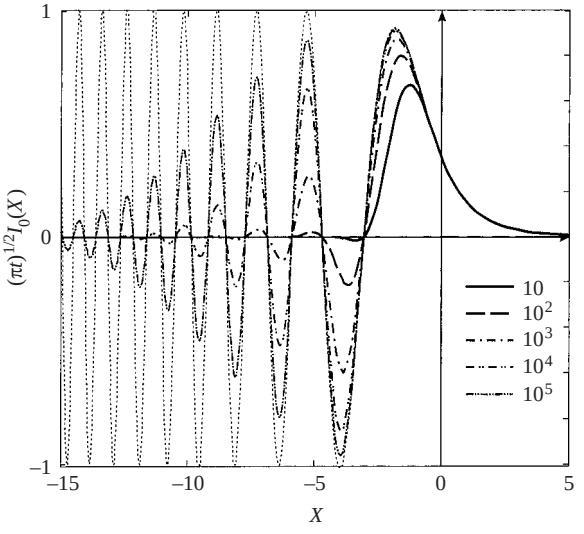

FIGURE 3. $(\pi t)^{1/2} I_0$ versus self-similar variable X for different times t (indicated in the figure). $(\pi t)^{1/2} I_0^{\varkappa=0}(X)$ is plotted as a dotted line as a reference curve.

For $\varkappa \neq 0$, to study large-t asymptotics of I_0 we apply the saddle point method. This is carried out in the Appendix; here we briefly discuss the results.

With a good accuracy I_0 can be presented as a product of the already studied $I_0^{\varkappa=0}$ and the damping factor (4.11), i.e.

$$I_0 = \frac{1}{\sqrt{2\pi t}} g\left(\frac{X}{\sqrt{2\pi}}\right) \exp\left(\frac{\varkappa X^3}{8t^{1/2}}\theta(-X)\right), \tag{4.16}$$

where $\theta(x)$ is the unit-step Heaviside function. Plots of normalized $I_0(X)$ for different times are shown in figure 3.

Having found I_0 we can easily evaluate all the family of integrals I_n from (4.16) and (4.9):

$$I_n \cong \frac{1}{(2\pi t)^{1/2+n/2}} \left[g^{(n)}\left(\frac{X}{\sqrt{2\pi}}\right) \exp\left(\frac{\varkappa}{8}\frac{X^3}{t^{1/2}}\theta(-X)\right) + O\left(\frac{1}{t^{1/2}}\right)\right], \tag{4.17}$$

where $g^{(n)}(Z) = \partial_Z^n g(Z)$. Thus, we have found all the formulae needed to describe the evolution of an arbitrary broadband perturbation. Below we investigate the main features of the evolution in detail.

4.2.4. *Extrema of the velocity field*

Of particular interest is behaviour of extrema of the velocity field described by I_0. Simplifying (4.16) for large negative X we obtain

$$I_0 \approx \frac{1}{\sqrt{\pi t}} \sin\left\{\frac{X^2}{4} + \frac{\pi}{4}\right\} \exp\left\{-\frac{\varkappa |X|^3}{8t^{1/2}}\right\}.$$

Maxima and minima are primarily determined by the trigonometric functions. Therefore it is easy to find approximately the location $X_{0,j}^{\mathrm{ext}}$ of the jth local extremum and the corresponding value of I_0, which we denote as $I_{0,j}^{\mathrm{ext}}$:

$$X_{0,j}^{\mathrm{ext}} \approx -\sqrt{\pi(4j+1)}, \qquad I_{0,j}^{\mathrm{ext}} \approx \frac{(-1)^j}{\sqrt{\pi t}} \exp\left\{-\frac{\varkappa \left|X_{0,j}^{\mathrm{ext}}\right|^3}{8t^{1/2}}\right\}. \tag{4.18}$$

We number the extrema starting with $j = 0$ for the front one. The main ($j = 0$) maximum of $I_0^{\varkappa=0}(X)$ is at $X_{0,0}^{\varkappa=0,\mathrm{ext}} \simeq -1.847$ with $I_{0,0}^{\varkappa=0,\mathrm{ext}} \simeq 0.521$. Although (4.18) are supposed to be valid for j not too small, the formulae provide a reasonably good description for all $j \geqslant 1$.

For finite $\varkappa$ every jth extremum ($j > 0$) grows until a time $t_{0,j}^{\mathrm{ext}}$

$$t_{0,j}^{\mathrm{ext}} = \frac{\varkappa^2 \left(X_{0,j}^{\mathrm{ext}}\right)^2}{64} = \frac{\varkappa^2 \pi (4j+1)}{64} \approx \frac{\varkappa^2 \pi}{16} j,$$

where it attains its maximum value

$$\max_t \left|I_{0,j}^{\mathrm{ext}}\right| = \frac{1}{\exp\left(\sqrt{\pi}\left(t_{0,j}^{\mathrm{ext}}\right)^{3/2}\right)} \sim \frac{64}{\exp\left(\pi^2 \varkappa^3 j^{3/2}\right)}$$

and then decays proportionally to $t^{-1/2}$: $I_{0,j}^{\mathrm{ext}} \approx (-1)^j/\sqrt{\pi t}$ as $t \to \infty$.

Note that for large t the impact of damping exponential factors in (4.16) on the first few extrema becomes negligibly small (see also figure 3 showing how the shape of the first maximum tends to the dotted reference curve corresponding to zero damping). The results looks strange at first sight, since in accordance with Shrira (1989) and Part 1 for each Fourier harmonic the effect of the Landau damping is $\sim \exp(-\mathrm{const} \times k^3 t^3)$ and thus is expected to be accumulating fast with time. The paradox is explained as follows: as time grows the first extrema are formed by longer and longer Fourier components which are just emerging out of their transition stage and begin their evolution as quasi-modes.

4.2.5. *Characteristic scales*

As $t \to \infty$ every extremum conserves its width in terms of the stretched variable X, while in terms of original physical coordinates it expands as $t^{1/2}$. The width of the first few extrema is of the order of unity (in terms of X) and decreases as $j^{-1/2}$ as j grows (see (A 12)). Thus we can introduce a dispersion lengthscale L_{disp} based upon the width of the first extrema:

$$L_{\mathrm{disp}} \sim t^{1/2}. \tag{4.19}$$

Parameter L_{disp}^{-1} describes the spatial frequency of oscillations of the QM part of the field. The value of L_{disp} is determined by the real part of the dispersion.

The second characteristic lengthscale determined by the Landau damping and denoted as L_{Landau} is the width of the QM zone (see § 4.2.2 above), i.e. the range of x where the QM perturbation is essentially non-zero is $t - L_{\text{Landau}} < x < t$:

$$L_{\text{Landau}} \sim \varkappa^{-1/3} t^{2/3}. \tag{4.20}$$

The ratio $L_{\text{Landau}}/L_{\text{disp}}$ gives the approximate number of the appreciable extrema in the perturbation. The number grows as $t^{1/6}$ as $t \to \infty$.

The third key lengthscale is the cut-off scale $k_{\text{Landau}}(t)$, i.e. the characteristic uppermost wavemumber of the disturbance which is determined by the damping factor (4.11):

$$k_{\text{Landau}} \sim \frac{1}{(\varkappa t)^{1/3}}.$$

Since the QM zone broadens as $t^{2/3}$ and the velocity field decays as $t^{-1/2}$ (for a monopole) due to the dispersion, then a straightforward estimate of the energy of the QM part of the perturbation yields

$$E_{\text{QM}} \sim L_{\text{Landau}} \langle u_{\text{QM}}^2 \rangle \sim t^{2/3}(t^{-1/2})^2 \sim t^{-1/3},$$

which coincides with (3.17).

4.2.6. *Forerunner*

Ahead of the perturbation front, i.e. for $x > t$, there is a small but non-zero part of the perturbation that we call 'forerunner'. The forerunner rapidly decays with the distance from the front. Taking the asymptotics of (A 10) for $X \gg 1$ and differentiating we find the main term:

$$I_0 \simeq \frac{2}{\pi X^3 t^{1/2}} = \frac{2t}{\pi(x-t)^3} = \frac{-2}{\pi \Delta v^3 t^2}, \tag{4.21a}$$

$$I_n \simeq \partial_x^n \frac{2}{\pi X^3 t^{1/2}} = \partial_x^n \frac{2t}{\pi(x-t)^3} = \frac{(3+n)!(-1)^{n+1}}{3\pi \Delta v^{3+n} t^{2+n}}. \tag{4.21b}$$

Far ahead the forerunner decays exponentially as $\sim \exp\{\varkappa X^3 t^{-1/2}/8\}$.

The origin of the phenomenon of the forerunner can be explained as follows. The initially localized perturbation in the vorticity field creates an algebraically decaying velocity perturbation. The perturbed vertical velocity w induces extra vorticity due to vertical displacement and the main flow vorticity gradient. This induced vorticity results in the slight perturbations of velocity field which constitute the forerunner.

4.3. *Long-wave initial perturbations*

Now consider the perturbations which are initially already long-wave. Assume the perturbation to be initially localized with the characteristic horizontal scale $\bar{L} \gg \bar{H}$ and its spectrum $\hat{u}_0(k)$ to be smooth. Then $\hat{u}_0(k)$ decays when k exceeds the characteristic wavenumber $k_L \sim L^{-1} \ll 1$.

First, similarly to § 4.2.2 we perform a preliminary analysis based on the group velocity. If we follow a point moving with a fixed velocity $v = x/t$ then for $\Delta v = 1 - v > 0$ (i.e. behind the front $v = 1$) we observe an oscillating pattern with a local wavenumber $k(v)$,

$$k(v) \cong \frac{\Delta v}{2},$$

with local amplitude

$$F \sim \left|\hat{u}_0\left(\frac{\Delta v}{2}\right)\right| \exp\left\{-\varkappa\left(\frac{\Delta v}{2}\right)^3 t\right\} \tag{4.22}$$

proportional to a product of two factors, both decaying as Δv grows. The first one rapidly decays if Δv exceeds $O(2L^{-1})$; the second one becomes effective when Δv exceeds $O(2(\varkappa t)^{-1/3})$. These 'cut-off' scales become of the same order at a timescale t_L specified by the relation $L^{-1} \sim (\varkappa t)^{-1/3}$,

$$t_L \sim L^3 \varkappa^{-3}. \tag{4.23}$$

Therefore at times small compared to t_L ($1 \ll t \ll t_L$) an intermediate asymptotics takes place and the perturbation behaves as a long-wave one: the QM zone where the perturbation is essentially non-zero is determined by its initial spectrum width $\Delta v_{\max} \sim L^{-1}$ and it broadens proportionally to t; the Landau damping can be neglected. At time $t \sim t_L$ both factors are important. At larger times, $t \gg t_L$, the Landau damping is the determining factor; the QM-zone broadening slows down to $t^{2/3}$ and the results of § 4.2 apply.

For example, if $\alpha_0 \equiv \int_{-\infty}^{+\infty} u_0(x,0)\,\mathrm{d}x \neq 0$ the field is proportional to $I_0(x,t)$. All the cases can be described by the following universal formula:

$$\psi_{\mathrm{QM}} \cong [U(z) - 1]\ a(x,t).$$

Here $a(x,t)$ is the amplitude factor ($a = -u_{\mathrm{QM}}(x,t)$):

$$a(x,t) \cong \begin{cases} u_0(x,0) * I_0^{\varkappa=0}(x,t), & 1 \ll t \ll t_L \\ u_0(x,0) * I_0(x,t), & t \sim t_L \\ \alpha_{n_{\min}} I_{n_{\min}}(x,t), & t \gg t_L, \end{cases}$$

where $*$ denotes convolution of two functions with respect to x:

$$f * g = \int_{-\infty}^{+\infty} f(x')g(x-x')\,\mathrm{d}x' = \int_{-\infty}^{+\infty} f(x-x')g(x')\,\mathrm{d}x' \tag{4.24}$$

and, as above, $n_{\min}$ is the minimal n such that $\alpha_n \neq 0$ (see (4.6)).

It is instructive to look at explicit formulae for some particular cases. For example, consider a perturbation with the Gaussian initial spectrum

$$\hat{u}_0(k) = \exp(-L^2k^2).$$

The saddle point method gives (see Appendix, § A.2):

$$\psi_{\mathrm{QM}} \cong [U(z) - 1]\ I_0^{\varkappa=0}(X,t)\ \exp\left\{\left(\frac{\varkappa}{8}\frac{X^3}{t^{1/2}} - \frac{L^2}{4}\frac{X^2}{t}\right)\theta(-X)\right\}.$$

The values of the stretched coordinate X at which each of the factors results in an e-fold decay are

$$X_{\mathrm{Landau}} \sim 2\varkappa^{-1/3}t^{1/6}, \qquad X_L \sim 2L^{-1}t^{1/2}.$$

The threshold time t_L at which they become equal is found from

$$X_\varkappa \sim X_L \Rightarrow t \sim L^{1/3}\varkappa^{-1/3} = t_L.$$

The specificity of each initial perturbation manifests itself in the dependence of the threshold time t_L on L and $\varkappa$ where the intermediate asymptotics becomes the generic asymptotics determined by the Landau damping.

4.4. *Vorticity evolution*

The evolution of the vorticity field, which is of independent interest, differs qualitatively from the evolution of any velocity components: its consideration cannot be confined to the quasi-mode dynamics.

4.4.1. *General formulae*

The vorticity perturbation due to the QM part is proportional to the velocity perturbation studied above and is therefore given by

$$\omega_{\mathrm{QM}} \cong U''(z)\,\alpha_{n_{\min}}\, I_{n_{\min}}(x,t),$$

where $n_{\min}$, as above, is the minimal n such that $\alpha_n \neq 0$ (see (4.6)).

However, the vorticity due to the non-modal part, primarily due to the tail, is essential. From the results of Part 1 it follows that for large times ($|k|\,t \gg 1$) the kth wave component of vorticity takes the form

$$\hat{\omega}_{\mathrm{Tail}} \simeq \hat{B}(k,z)\,\mathrm{e}^{-\mathrm{i}kUt}, \quad \hat{B}(k,z) \simeq \hat{\omega}_0(k,z) + \frac{U''(z)}{U'(z)}\hat{u}_0(k,z). \tag{4.25}$$

To obtain the spatial distribution of the vorticity in the tail we have to take an integral of the type (3.11) in the limits $(-\infty, -k_1)$ and $(k_1, +\infty)$. However we can neglect the contribution of the initial transition range ($|k| < k_1$) for the same reasons as for the QM part in § 3. Then performing inverse Fourier transform we arrive at the simple explicit formula

$$\omega_{\mathrm{Tail}}(x,z,t) \simeq B(x-Ut,z) \equiv \omega_0(x-Ut,z) + \frac{U''}{U'}u_0(x-Ut,z). \tag{4.26}$$

The first term is due to advection of the initial vorticity by the main flow; the second one is the vorticity induced by vertical displacements, mainly at the initial stages of the evolution.

4.4.2. *Vorticity in the 'tail-zone'*

According to (4.26) ω_{Tail} is localized along the line $x = U(z)t$ with horizontal width of order L, i.e. the scale of the initial perturbation. In the QM zone this line is close to the surface: $x \simeq (1-z)t$ ($\bar{x} \simeq (\bar{U}_s + \bar{U}'_s)\bar{t}$) or $z_{\mathrm{Tail}}(x,t) = (t-x)/t \equiv \Delta v$. The amplitude of the vorticity remains of the same order and is localized in a a comet-tail-like domain: a slightly oblique strip having constant horizontal cross-section and vertical one narrowing with time:

$$\Delta x_{\mathrm{Tail}} \simeq L, \quad \Delta z_{\mathrm{Tail}} \simeq \frac{L}{t}.$$

We will call this region the 'tail-zone'. It is in this tail-zone where the non-modal part always dominates since the vorticity of the QM part decays as $t^{1/2}$ ($t^{n/2+1/2}$ for n-pole). The vorticity distribution in the tail zone is sketched in figure 4.

It is also interesting to compare vorticity and enstrophy averaged over the vertical coordinate. For the non-modal part we have

$$\int_0^\infty \omega_{\mathrm{Tail}}\,\mathrm{d}z \sim \omega_0\,\Delta z_{\mathrm{Tail}} \sim t^{-1}, \qquad \int_0^\infty \omega_{\mathrm{Tail}}^2\,\mathrm{d}z \sim \omega_0^2\,\Delta z_{\mathrm{Tail}} \sim t^{-1}.$$

For the QM part we find the following estimates:

$$\int_0^\infty \omega_{\mathrm{QM}}\,\mathrm{d}z \sim t^{-1/2} \quad \left(\sim t^{-n/2-1/2}\right), \quad \int_0^\infty \omega_{\mathrm{QM}}^2\,\mathrm{d}z \sim t^{-1} \quad (\sim t^{-n-1}).$$

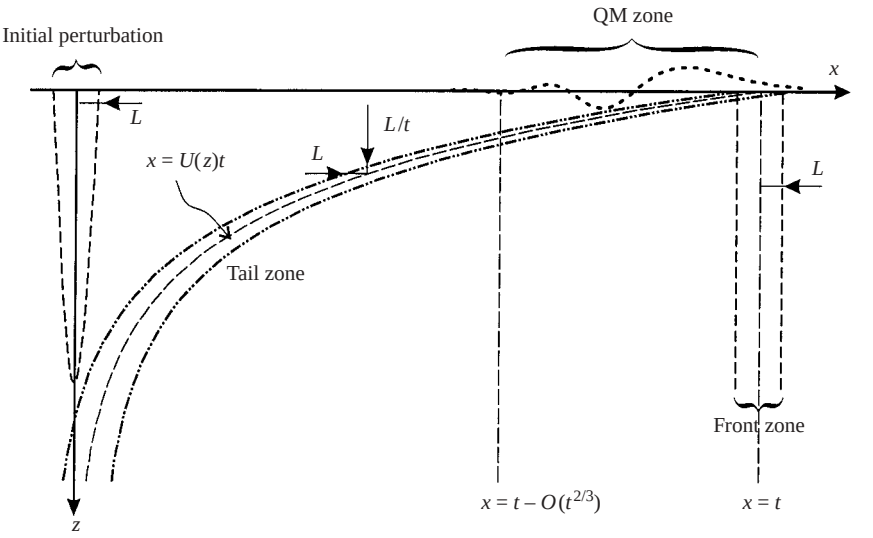

FIGURE 4. Sketch of the solution spatial structure at large t. The strip where the tail-zone vorticity is localized is shown by a dot-dashed line; the QM zone, the front zone and the region of initial perturbation are depicted by dashed lines.

Note that in terms of *averaged vorticity* the QM part dominates in the case of a monopole.

The tail-zone 'touches' the surface in the relatively narrow region near the front of the perturbation: $t - x \sim L$ (recall that $t \gg L$). In terms of X and z the size of this region is $X \sim Lt^{-1/2}$, $z = \Delta v \sim Lt^{-1}$. We will call it the 'front zone'.

Behind the front zone, the local critical layer z_c, i.e. the layer where the local phase velocity of the quasi-mode matches the basic flow velocity, is at half the distance $z_c \simeq \Delta v/2 \cong z_{\mathrm{Tail}}/2$ between the surface $z = 0$ and the localization of the tail zone: $z_{\mathrm{Tail}} \simeq \Delta v$ where the local group velocity coincides with the velocity of the mean flow.

4.4.3. *Velocity distribution in the tail zone*

Narrowing of the tail zone (in the vertical direction) results in a decrease of the amplitude of all the velocity components. We focus on the u component as the most important for long-wave perturbation. Using the relation $\omega \simeq -\partial_z u$ approximately valid for long-wave perturbations we obtain

$$u_{\mathrm{Tail}} \simeq \int B(x - U(z)t, z)\,\mathrm{d}z. \tag{4.27}$$

Since the vorticity ω is localized in a thin layer the velocity u_{Tail} varies fast in this layer. We introduce a fast vertical coordinate referenced from the depth of the tail:

$$z = z_{\mathrm{Tail}} + Z/t.$$

(The vorticity is very small if $|Z| \gg 1$.) Then the first argument in the integrand can be simplified to

$$x - U(z)t = x - U(z_{\mathrm{Tail}} + Z/t)t \approx [x - U(z_{\mathrm{Tail}})t] - U'(z_{\mathrm{Tail}})Z \approx Z$$

as the terms in brackets are zero and $U'(z_{\mathrm{Tail}}) \approx -1$ when the layer is not too deep. Thus we have

$$u_{\mathrm{Tail}} \simeq \frac{1}{t} \int B(Z, z_{\mathrm{Tail}})\, \mathrm{d}Z.$$

In the case of a monopole we see that the total variation of u_{Tail} is not zero, hence the tail zone serves as a boundary between zero and non-zero horizontal velocity. In the case of a multipole the velocity u_{Tail} is localized in the tail zone, since the integral $\int_{-\infty}^{+\infty} B(x, z)\, \mathrm{d}x = 0$. In the case of a dipole ($n_{\min} = 1$) we have a jet, and in the case of quadrupole a jet with a counter-jet, etc. The velocity in all cases is of the same order: $O(t^{-1})$. However, for a monopole the velocity is distributed in the area linearly stretching with time (the length is the length of the tail), so the energy decays as t^{-1}, since $t\,O(t^{-1})^2 = O(t^{-1})$. For higher multipoles the velocity is localized in the area-preserving region and the energy of the tail part decays as $O(t^{-2})$, that is in accordance with our previous rough estimations.

Although the velocity in the tail decays faster than in the QM part for monopole perturbations ($\alpha_0 \neq 0$) for which it decays as $t^{-1/2}$, these manifestations of initially localized perturbations might be of independent interest because of their unusual spatio-temporal structure discussed above. The tail tends to the so-called vorticity patch known for its highly non-trivial dynamics and important role in many processes (Saffman 1994), although in our case the patch strength is probably too weak to expect it to play an important role.

Consider an example: let an initial perturbation be localized in an ellipse with semi-axes L and D with its maximum at $z = h$ as sketched in figure 1, with the Gaussian distribution of vorticity:

$$\omega_0 = \omega_{\max} \exp\left(-\frac{x^2}{L^2} - \frac{(z-h)^2}{D^2}\right). \tag{4.28}$$

Using Fourier transform with respect to x it is easy to show that

$$\int u_0(x, z)\, \mathrm{d}x = \frac{\pi}{2} L D \omega_{\max}\, \mathrm{erfc}\left[\frac{z-h}{D}\right], \quad \int \omega_0(x, z)\, \mathrm{d}x = L\sqrt{\pi}\omega_{\max} \exp\left[-\frac{(z-h)^2}{D^2}\right].$$

Also, let $U = \exp(-z)$, then $U''/U' \equiv -1$. Then from (4.27) we have

$$u_{\mathrm{Tail}} \simeq \frac{L\omega_{\max}}{t} \left\{ \sqrt{\pi} \exp\left[-\frac{(\Delta v - h)^2}{D^2}\right] - \frac{\pi}{2} D\, \mathrm{erfc}\left[\frac{\Delta v - h}{D}\right] \right\} \theta(\Delta v - z).$$

Recall that Δv is specified by x and t as $\Delta v = (x - t)/t$ and thus u_{Tail} varies slightly along x at the distances under consideration.

Generalizing the above formula we can suggest an estimate for an arbitrary generic perturbation of horizontal lengthscale $L \not\ll 1$:

$$u_{\mathrm{Tail}} \sim \frac{L\omega_{\max}}{t} \theta(\Delta v - z).$$

Parameter D does not enter into the estimate since we consider the perturbations for which it is of order of unity.

4.5. *QM dominance revisited*

Having clarified the main features of perturbation field evolution, now it is useful to revisit the issue of how the QM dominance should be defined. On the basis of the established picture of field evolution it is possible to introduce new criteria for the dominance and to re-assess, depending on the criterion used, when the QM are

prevalent. In § 3 we employed crude *global* criteria, i.e. we required the quasi-mode to be so dominant that its total energy *averaged over entire perturbed domain* should far exceed the non-modal part of the perturbation. For most conceivable applications the more natural criteria would be some *local* ones based upon field characteristics averaged either over the QM zone, which is the only place where an essentially non-zero velocity field is present, or over the main extremum of the field.

4.5.1. *The 'initial transition' component*

We begin with the essentially non-local wave part $\psi_{\rm Ini}$ formed by the longest wave components which are at the initial stage. We cannot describe the evolution of this part since we have no closed-form formulae for this stage of the evolution of the harmonic perturbation. Here we show that for $t \gg 1$ the $\psi_{\rm Ini}$ part becomes small compared to the QM part.

We estimate a characteristic amplitude of this part and its lengthscale, utilizing the fact that the wave components at the initial stage preserve the same order of magnitude:

$$\hat{\psi}(k, z, t) \sim \hat{\psi}(k, z, 0) \equiv \hat{\psi}_0(k, z).$$

We also approximate $\hat{\psi}_0(k, z)$ for small k by the main term in its Taylor expansion:

$$\hat{\psi}_0(k, z) \simeq \hat{\psi}_0^{(n)}(0, z)(\mathrm{i}k)^n,$$

where $\hat{\psi}_0^{(n)} \equiv \partial^n \hat{\psi}_0 / \partial(\mathrm{i}k)$ and n should be understood as $n_{\min}$.

Introduce a low-pass filtering function $\hat{\phi}(k)$ rapidly decaying for $|k| > k_{\rm L} = 1$. Then its x-space image $\phi(x) = (2\pi)^{-1} \int_{-\infty}^{+\infty} \hat{\phi}(k) \exp(\mathrm{i}kx)\,\mathrm{d}x$ decays if $|x| > x_{\rm L} = 1$. We do not specify the filtering function. It can be smooth (Gaussain, Lorentz) or, say, rectangular. Assuming ($k_{\rm L} \propto t^{-1}$) we, in the case in hand, use a narrowing filter function: $\hat{\phi}(tk)$.

Using the substitution $k' = kt$, $x' = x/t$ we can estimate $\psi_{\rm Ini}$ as follows:

$$\psi_{\rm Ini} \simeq \frac{1}{2\pi} \int_{-\infty}^{+\infty} \hat{\psi}(k, z, t)\, \hat{\phi}(kt) \mathrm{e}^{\mathrm{i}kx}\,\mathrm{d}k \sim \frac{\hat{\psi}_0^{(n)}(0, z)}{2\pi} \int_{-\infty}^{+\infty} (\mathrm{i}k)^n\, \hat{\phi}(tk) \mathrm{e}^{\mathrm{i}kx}\,\mathrm{d}k$$
$$= \frac{\hat{\psi}_0^{(n)}(0, z)}{2\pi t^{1+n}} \int_{-\infty}^{+\infty} (\mathrm{i}k')^n\, \hat{\phi} \mathrm{e}^{\mathrm{i}k'x'}\,\mathrm{d}k' = \frac{\hat{\psi}_0^{(n)}(0, z)}{2\pi t^{1+n}} \phi^{(n)}(x/t),$$

where $\phi^{(n)}(x) = \partial_x^n \phi(x)$ is a function decaying when $|x| > x_{\rm L} = 1$.

From (4.29) it is easy to see that the initial transition part decays as t^{-1} (t^{-1-n}) and spreads as t. The horizontal velocity decays as the stream function and the vertical velocity decays as t^{-2-n}.

The total energy of this part of the perturbation decays as $E_{\rm Ini}(t) \sim t\,(t^{-(1+n)})^2 = t^{-1-2n}$, which is the same as (3.20). Since this energy is uniformly distributed over the perturbed area, it is straightforward to find its parts in the QM zone and in the area of the global maximum, which yields the estimates $t^{-4/3-2n}$ and $t^{-3/2-2n}$, respectively.

4.5.2. *Local estimates of the QM and tail components*

To compare energy and velocity in the region of the main (global) extremum for an arbitrary multipole we need to carry out an analysis of I_n given by (4.17) similar to that in § 4.2.4. From (4.17) it is easy to find asymptotics of I_n for large negative X:

$$I_n \approx \frac{1}{\sqrt{\pi t}} \frac{X^n}{2^n t^{n/2}} \sin^{(n)} \left\{ \frac{X^2}{4} + \frac{\pi}{4} \right\} \exp\left\{ -\frac{\varkappa |X|^3}{8t^{1/2}} \right\}, \tag{4.29}$$

where $\sin^{(n)}(x) \equiv \mathrm{d}^n \sin x/\mathrm{d}x^n$. At the leading order the position of jth extremum $X^{\mathrm{ext}}_{n,j}$ is determined by the trigonometrical function in (4.29) while the corresponding extremal value $\left|I^{\mathrm{ext}}_{n,j}\right|$ is found by substituting $X^{\mathrm{ext}}_{n,j}$ into (4.29):

$$X^{\mathrm{ext}}_{n,j} \approx -\sqrt{\pi(4j+(-1)^n)} \approx \sqrt{4\pi j}, \tag{4.30a}$$

$$\left|I^{\mathrm{ext}}_{n,j}\right| \approx \frac{1}{2^n \pi^{1/2}} \frac{(4\pi j)^{n/2}}{t^{n/2}} \exp\left\{-\frac{\varkappa(4\pi j)^{3/2}}{8t^{1/2}}\right\}. \tag{4.30b}$$

For $n \neq 0$, in contrast to the case of I_0 the global extremum does not coincide with the first maximum, unless time is not too small, but with one of the last extrema in the QM zone. Differentiating (4.30) with respect to j and equating it to zero we find the particular number j specifying the global extremum:

$$j^{\mathrm{main}}_n = \frac{n^{2/3} t^{1/3}}{(3\varkappa)^{2/3}\pi}. \tag{4.31}$$

By virtue of (4.30) the main (global) extremum of I_n is

$$\left|I^{\mathrm{main}}_n\right| \approx \frac{n^{n/3} t^{-1/2-n/3}}{\sqrt{\pi}(3\varkappa)^{n/3}} \exp\left\{-\frac{n}{3}\right\},$$

which occurs in the vicinity

$$X^{\mathrm{main}}_n \approx \sqrt{4\pi j^{\mathrm{main}}_n} = \frac{4n^{1/3}}{(3\varkappa)^{1/3}} t^{1/6},$$

$$x^{\mathrm{main}}_n \approx t - \frac{4n^{1/3}}{(3\varkappa)^{1/3}} t^{1/6+1/2} = t - \frac{4n^{1/3}}{(3\varkappa)^{1/3}} t^{2/3},$$

$$v^{\mathrm{main}}_n \approx \frac{4n^{1/3}}{(3\varkappa)^{1/3}} t^{-1/3}.$$

The energy averaged over the global maximum can be estimated as the product of maximal energy density and the duration of the maximum, i.e.

$$t^{1/2} |u^{\mathrm{main}}|^2.$$

The estimate of the energy density for the non-modal part (of which the energy in the tail-part is the main constituent) remains the same as in § 3 but the total non-modal energy $\widehat{E}_{\mathrm{Tail}}$ in the domain of interest (the main extremum) is much smaller than the previous estimate E_{Tail} because of the smaller size of the zone: $\widehat{E}_{\mathrm{Tail}} = E_{\mathrm{Tail}} t^{-1/2}$.

Similarly, if we wish to compare the energy of modal and non-modal parts in the QM zone only, which spreads as $t^{2/3}$ (rather than as $O(t)$), we find $\widehat{E}_{\mathrm{Tail}} = E_{\mathrm{Tail}}\, t^{-1/3}$.

If we compare the evolution of the perturbation energy in the modal and non-modal parts of the field averaged respectively over the entire perturbed domain, the QM zone or the main extremum we find that although in all cases the corresponding energies behave as t^{ν} the exponents are different in different cases. The results are summarized in table 2.

Here the first five multipoles and three different criteria based on energy are considered. For each n the exponents ν corresponding to the modal and non-modal parts of the field as well as to their ratio are presented. It worth noting that the two local criteria lead to almost identical results (presented in the last six columns),

	Total energy			QM zone			Main maximum		
	QM	Tail	Ratio	QM	Tail	Ratio	QM	Tail	Ratio
n	$-\frac{1}{3}-\frac{2}{3}n$	ν_{Tail}		$-\frac{1}{3}-\frac{2}{3}n$	$\nu_{\text{Tail}}-\frac{1}{3}$		$-\frac{1}{2}-\frac{2}{3}n$	$\nu_{\text{Tail}}-\frac{1}{2}$	
0	$-1/3$	-1	$2/3$	$-1/3$	$-4/3$	1	$-1/2$	$-3/2$	1
1	-1	-2	1	-1	$-7/3$	$4/3$	$-7/6$	$-5/2$	$4/3$
2	$-5/3$	-2	$2/3$	$-5/3$	$-7/3$	1	$-11/6$	$-5/2$	$2/3$
3	$-7/3$	-2	$-1/3$	$-7/3$	$-7/3$	0	$-15/6$	$-5/2$	0
4	-3	-2	-1	-3	$-7/3$	$-2/3$	$-19/6$	$-5/2$	$-2/3$

TABLE 2. Comparison of the evolution of the perturbation energy in the modal and non-modal parts and their ratio averaged over the entire perturbed domain, the QM zone or the main extremum.

n	0	1	2	3	4
Total energy	$2/3$	1	$2/3$	$-1/3$	-1
Energy in the QM zone (or in the main extremum)	1	$4/3$	1	0	$-2/3$
Horizontal velocity in the main extremum	$1/2$	$1/3$	0	$-1/3$	$-2/3$

TABLE 3. Comparison of ratios of energy in the QM zone and horizontal velocity in the main extremum.

while differing noticeably from the crude global energy estimates of § 3. The latter for convenience are reproduced in the first three columns. The main advantage that the local criteria provide is that the 'adjustment' times defined on their basis are much shorter and, we believe, more realistic. It is also worth noting that by using the local criteria the QM asymptotics occur for the octapoles ($n = 3$) as well.

As an alternative to the energy criteria it is possible to use criteria based on longitudinal velocity. If we choose as the criterion a local one based on the QM prevalence in the u-component of velocity within the main extremum $u^{\max}$ then it is straightforward to calculate $u^{\max}_{\text{QM}}$ and $u^{\max}_{\text{non-modal}}$. The comparison of ratios $\log(|u^{\max}_{\text{QM}}|/|u^{\max 1}_{\text{non-modal}}|)$ and $\log(E_{\text{QM}}/E_{\text{non-modal}})$ based on the global and local criteria is presented in table 3.

Thus in terms of u the QM prevalence begins later for monopoles and dipoles and does not happen at all for octapoles. Although, again, strictly speaking, we can claim only the fact that our estimates do not show such a prevalence for $n \geqslant 4$. The possibility that the QM dominance holds for $n \geqslant 4$ cannot be excluded. The specific choice of the criterion is dictated by the particular problem: the point we would like to emphasize here is that whatever the choice the QM asymptotics does prevail in most cases of interest corresponding to $n = 0$ or $n = 1$.

4.6. *Direct simulation of the evolution*

The picture of small perturbation evolution found above analytically obviously requires numerical testing and raises a number of questions which can be addressed only by means of direct numerical simulation. The following questions we view as fundamental:

Is the qualitative picture of evolution we arrived at adequate or, more specifically, is the perturbation velocity field indeed dominated by the quasi-mode, while the vorticity is localized in the tail, being smeared in the comet tail?

Are the analytical results quantitatively correct and with what accuracy? Where do the theory shortcomings lie and what are the reasons behind them?

What are the characteristic times of 'adjustment' of an initial perturbation?

We try to address these questions by direct numerical simulation of a small number of examples.

Direct numerical simulation of the two-dimensional linear problem has been carried out by the pseudo-spectral method: Fourier expansion is performed with respect to x and Chebyshev polynomials are used to represent the solution with respect to z. The initial vorticity is set by a Gaussian distribution (4.28) with the parameters: $\omega_{\max} = 1$, $L = 2\pi$, $D = 1$, $h = 0$, i.e.

$$\omega_0 = \exp\left(-z^2 - \frac{x^2}{4\pi^2}\right). \tag{4.32}$$

The basic flow is the Falkner–Skan flow (Part 1; Dupont & Caulliez 1993). The evolution of this particular initial perturbation is the test case we have chosen. Results of the evolution taken at a rather arbitraryily chosen moment $t = 1000$ are shown in figure 5(a, b) where the spatial distributions of the instantaneous vorticity and velocity (ψ-function) fields are presented. The results confirm the main features of the qualitative picture of evolution established analytically: in the vorticity distribution shown in figure 5(a) the tail zone is very pronounced and has the predicted comet tail shape, while in the ψ distribution shown in figure 5(b) only the QM part with its characteristic oscillations can be seen. Notice that there is no evidence of a singularity in the critical layer for the QM part with a local wavenumber, i.e. at half the distance between the tail zone and the surface (see above).

The next step is to compare quantitatively our analytical results with numerics. To this end we choose to use the surface value of the horizontal velocity as a useful and convenient field characteristic. It can be found as $u_s = -\partial_z \psi|_{z=0}$. At the same time u_s can be easily extracted from the analytical results:

$$u_s = \int_{-\infty}^{+\infty} u_s(t=0)\, I_0(x, z)\, \mathrm{d}x,$$

where $\int_{-\infty}^{+\infty} u_s(t=0)\, \mathrm{d}x$ is the amplitude of the initial Dirac's delta function. It equals $2\pi^2$ for initial perturbation (4.32). The integral

$$I_0 = (2\pi)^{-1} \int_{-\infty}^{+\infty} \exp(\mathrm{i}k(x - c_p(k)t)\, \mathrm{d}k$$

can be evaluated by both a numerical (FFT) method and analytically (by the saddle point method). The latter approach is based on the long-wave approximation of $c_p(k)$ and gives the useful formula (4.16). Applying the FFT method we again have two options: we can use either the long-wave asymptotics for $c_p(k)$ or its 'numerically exact' behaviour computed in Part 1, § 5; below for brevity we will use the word 'correct' for the latter. The above four approaches were used, and the results are presented in figure 6. The fundamental question we are interested in now is to check to what extent the QM part of the field is indeed sufficient to describe velocity field evolution. Comparing the results of the numerical FFT integration of I_0 using the correct behaviour of $c_p(k)$ (curve 2) to the direct simulation (curve 1) we can see that the curves nearly coincide: both the positions of the maxima and their values are described perfectly. Curves 3 and 4 also almost coincide. Being both based on the use of the same long-wave expansion of $c_p(k)$, curve 3 shows results of numerical FFT integration of I_0, while curve 4 gives its evaluation by the saddle point method.

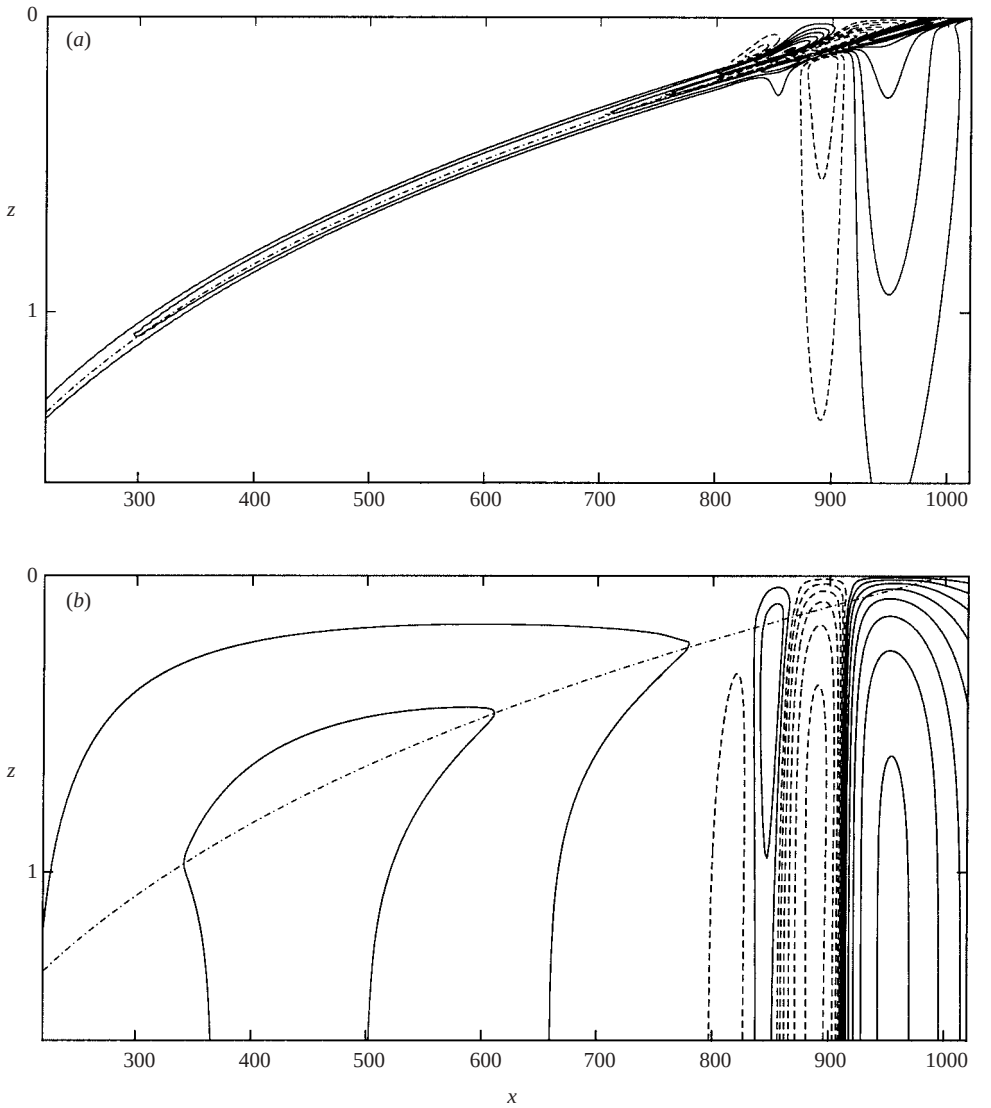

FIGURE 5. Example of numerically simulated spatial distribution of the perturbation field at $t = 1000$ evolved from initial conditions (4.32). (*a*) Vorticity isolines $\omega(x, z, t = 1000)$. Solid (dashed) curves are for positive (negative) values of vorticity. Dot-dashed line indicates the centre of the tail zone: $x = Ut$. (*b*) Stream function isolines: $\psi(x, z, t = 1000)$. Solid (dashed) curves are for negative (positive) values of ψ. Dot-dashed line indicates the centre of the tail zone: $x = Ut$.

The importance of this observation is that it demonstrates the excellent performance of the saddle point approach. A discrepancy in the positions of maxima between the two pairs of curves, negligible for the main one and increasing with the distance from the front, is obviously due to the long-wave approximation of the dispersion adopted for curves 3 and 4. The increase in separation between the two pairs of curves is easy to explain: since the maxima with the greater j are formed by shorter local wave components for which the difference between the true and long-wave c_p is greater, the discrepancy also grows. Nevertheless, the use of this approximation gives reasonable

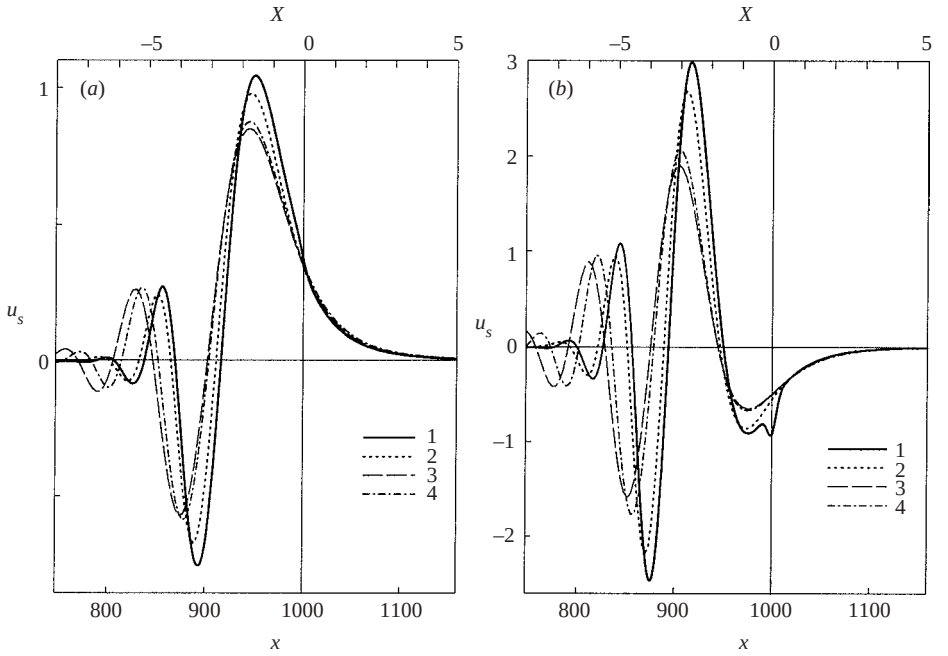

FIGURE 6. Normalized surface horizontal velocity u_s for $t = 1000$ evolved from initial conditions: (*a*) (4.32) and (*b*) $\partial_x \omega_0$. u_s is normalized by $(\pi t)^{-1/2} \int_{-\infty}^{+\infty} u_s(t = 0)\,\mathrm{d}x$ and $(\pi t)^{-1} \int_{-\infty}^{+\infty} (-x u_s(t = 0))\,\mathrm{d}x$ in (*a*) and (*b*), respectively. Curve 1 represents direct two-dimensional numerical simulation; curves 2, 3, 4 describe only QM part: 2 – FFT method for the true dispersion with $c_p(k)$ calculated numerically; 3 – FFT method for the long-wave approximation of $c_p(k)$; 4 – asymptotic formula (4.16).

accuracy for the positions of the front and the first few maxima, while the amplitudes of all extrema are described quite well. The presence of the field non-modal part can be detected only in the plot of the dipole evolution, where it manifests itself as a blip in curve 1, at the point where the tail reaches the surface (see figure 4). The variation of the pulse width L does not change anything in this context. The overall conclusion we arrive at is that the analytical approach based on long-wave approximation developed here and the saddle point evaluation of the integrals gives a quite satisfactory accuracy.

We present one more figure illustrating the emergence of the QM asymptotics by plotting the maximum of the horizontal velocity at the surface evolving from initial conditions (4.32) with $L = 2$ as function of time (see figure 7). Other parameters and the flow are the same as in the previous figure. In accordance with the analytical formulae the curve does indeed tend to $t^{-1/2}$ and the precision of this asymptotics increases with time.

Summarizing the above simulations we can conclude that the qualitative picture of the evolution found analytically is adequate. Indeed, for large times the perturbation velocity field is dominated by the quasi-mode, the vorticity being localized in a long and narrow strip. Moreover, the analytical results proved to be quantitatively correct with a good accuracy. Concerning the insignificant discrepancies found, it is easy to explain the shifts of the extrema positions by the approximation of the dispersion relation $c(k)$ adopted.

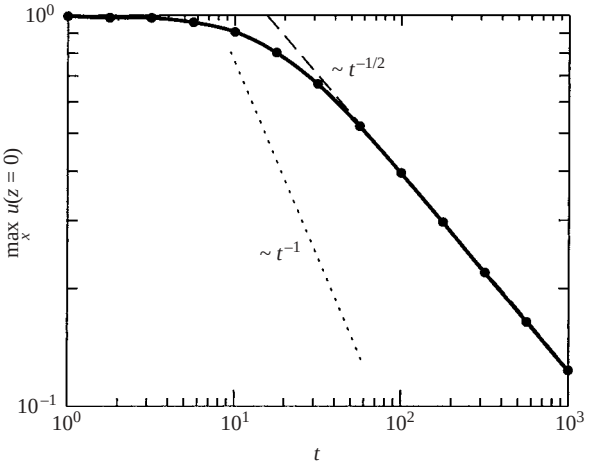

FIGURE 7. Decay of the maximal horizontal velocity at the surface evolving from initial conditions (4.32) with $L = 2$. Dashed line shows the slope $t^{-1/2}$ corresponding to the QM decay. Dotted line indicates the law of the large-time decay of the non-modal part.

An investigation of the characteristic times of 'adjustment' as a function of the parameters of the initial perturbation, which is obviously needed, requires, in our view, a separate study for the following reasons. First, separation of the QM and non-quasi-mode parts is far from straightforward in a numerical simulation. A possible way to address this problem would be to construct the separation based upon the specificity of the vertical structure of different parts of the solution. However, such a procedure, if applied, would make the simulations quite cumbersome. Moreover, even for the perturbations of the same initial shape the parameter space is two-dimensional (L and D) and merely taking a sufficient number of points requires a very computer intensive simulation. If the shape is varied as well, the required simulations would grow to an industrial scale.

5. Concluding remarks

The main advance in understanding we report in the present paper is captured by the term 'adjustment', a term we introduced to describe the key feature of the evolution of arbitrary broadband initially localized inviscid two-dimensional perturbations in boundary layer flows without inflection points. We found that the evolution of an arbitrary† localized perturbation exhibits two qualitatively distinct stages or regimes: the second stage corresponds to slow dynamics of long-wave perturbations, which is well described in terms of quasi-mode evolution; the first stage involves Fourier components of all scales and corresponds to a relatively fast transitional process resulting in the disappearance of the short scales. The fact that there is a universal asymptotic regime free of short and medium scales enables us to refer to the corresponding transitional process by the term 'adjustment'.

† Here the term 'arbitrary' is used in the following sense: the initial perturbation can be composed of harmonics of arbitrary horizontal scales in x; the vertical scale is assumed to be of the order of the boundary layer thickness, while the shape is such that at least one of the first three moments is non-zero in accordance with the conditions formulated in § 3 and § 4.5.

The emergence of the quasi-mode as the universal asymptotics is quite counter-intuitive, since for each of the constituent Fourier components considered separately the quasi-mode regime occurs just for a fraction of them and only as an intermediate asymptotics. The explanation is based on the observation that the bounds of the spectral interval exhibiting quasi-mode behaviour evolve with time in a specific way, while the relatively smaller scale non-quasi-mode components prove to be rapidly decaying. Although unable to describe the adjustment itself, we constructed a few rough estimates showing when and in what sense the contribution of the non-quasi-mode part can be considered negligible. We emphasize that the derived long-time quasi-mode asymptotics are explicitly expressed in terms of certain integrals of the initial distributions. Since the quasi-mode asymptotics essentially overlaps with the triple-deck one, the above implies that the triple-deck regime which is applicable only for long-wave initial perturbations also represents the large-time asymptotics of arbitrary broadband ones.

The quantitative results which follow from the dominance of the QM asymptotics have profound importance. In particular, the $t^{-1/2}$ horizontal velocity decay ensures that, as will be shown in the next paper of the series, the nonlinear effects are 'accumulated' and grow despite the amplitude decay. The overall qualitative picture of evolution derived, which includes the emergence of a vortex patch due to the non-QM part, might also have important implications, primarily in the context of nonlinear dynamics and especially of periodic perturbations.

Since so far the only attempt to tackle analytically broadband perturbations was based on the use of a piecewise linear model by Bowles & Smith (1995), it seems worthwhile to compare the results and discuss briefly the similarities and differences which are illuminating. In § 6 of Part 1 we discussed in some detail the relationships between the decaying quasi-modes in smooth continuous models of boundary layers and neutral discrete modes of piecewise linear models for monochromatic perturbations, which prepares the ground for a discussion of broadband packets. Following Part 1 we will refer to the particular piecewise linear approximation of the basic flow which has one break as the PL_1 model. Figure 8 presents a typical sample of a simulation of the evolution of a Gaussian pulse in smooth and PL_1 models of boundary layer. The PL_1 model performs remarkably well in predicting the position of the front for all times and shape of the first field extremum at large times. The adequate prediction of the front position is not surprising since it has long been known that in the long-wave limit the real part of dispersion relation for the PL_1 profile approximates well that of the true dispersion relation. The good prediction of the magnitude at the front at large times and not so good for intermediate scales is due to the fact that, as was mentioned in § 4.2.4, as time increases the first extremum is formed by longer and longer components and so the effect of the Landau damping on the vicinity of the front is decreasing. The shortcomings of the piecewise model and the underlying reasons are quite obvious. The model fails completely to describe the field outside the vicinity of the front and its global structure, since it is the Landau damping which is responsible for the cut-off of the shorter scales and formation of the rear front of the perturbation. The PL_1 model greatly overestimates the role of shorter scales,† and wrongly predicts the position and the magnitude of the field maximum. By differentiating once the curves presented in figure 8 with respect to x one obtains the

† The integral energy of perturbations is preserved in the model while in reality the energy decays as $t^{-1/3}$ because of the disappearance of short and medium scales.

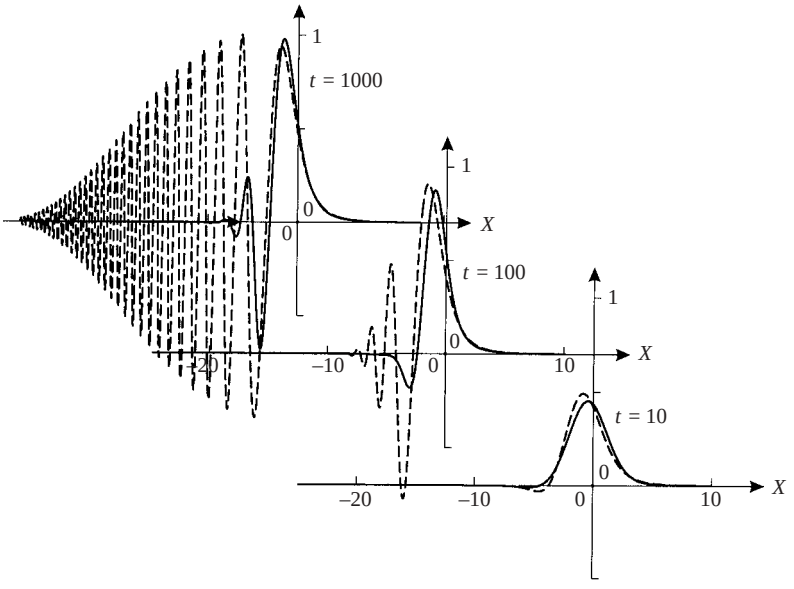

FIGURE 8. Evolution of a broadband Gaussian initial pulse (4.31) ($L = 2\pi$, $D = 1$, $h = 0$): normalized surface velocity $\tilde{u}_s = u_s\sqrt{\pi t}(\int_{-\infty}^{+\infty} u_s(t=0)\,\mathrm{d}x)^{-1}$ vs. self-similar coordinate X in a smooth (Falkner–Skan) boundary layer (solid) and the fitted piecewise linear profile with one break (dashed).

picture of evolution for the initial distributions of the dipole type: the PL_1 model predictions lose any resemblance to the true picture, except for the position of the front. We conclude, that the PL_1 model can indeed be used to find the position of the front, and, with caution, for times large enough, to describe the field structure at the front. Because of the strong presence of parasitic scales, the model, despite the tempting simplicity, cannot be used for any nonlinear analysis. As shown in Part 1, an increase in the number of breaks would make the situation worse. However, if the PL_1 model were amended by taking into account Landau damping in the spirit of the example discussed in Part 1, § 6, it would give a qualitatively, and even quantitatively, adequate picture of the evolution. The issue merits further investigation.

Although the main potential applications and developments of our linear results lie in the area of nonlinear dynamics, there is a plenty of room for improvement and further development even remaining within the framework of the linear theory. First, within the framework of the same problem statement the integral estimates concerned with the non-modal part of the perturbation could be improved, which would result in a better idea of the characteristic times of adjustment. Further improvement of evaluation of the transitional period can be also achieved by extensive numerical simulations. In particular, the so far unknown dependence on the parameters of the initial perturbations could be established. The reserves of the analytical approach do not seem to be exhausted either. Perhaps, analytical solutions for particular boundary layer profiles and particular initial distributions can be developed. We made no serious attempt to explore this direction, although, because of the universality of the perturbation evolution found, even a single example of this kind would be very helpful.

The present study was confined to spatially uniform steady boundary layers. There is no doubt that the phenomenon of the QM dominance in the long-time asymptotics

holds for a wide class of spatially inhomogeneous and non-stationary boundary layers, although to specify this class and to find the analogues to the homogeneous asymptotics $t^{-1/2}$ is a formidable problem in a general setting. However, now we just point out that if the scales of inhomogeneity and non-stationarity admit the WKB approximation, which is very often the case, then a direct generalization of the results is quite straightforward.

Although studying the effects of nonlinearity, viscosity and three-dimensionality lies beyond the scope of the present paper, it seems appropriate to outline how the results obtained could help in understanding these questions. In the most of the situations of interest the nonlinearity and viscosity are weak and, therefore, their effects become important only after being accumulated over sufficiently large times. The two-stage evolution pattern revealed allows a dramatic simplification of the description. During the relatively fast adjustment both nonlinear and viscous effects can be safely neglected. At the stage of slow evolution, the description has been drastically simplified: instead of tracing the dynamics of a continuum of singular vertical modes of continuous spectrum of all horizontal scales present in the initial conditions, we reduce the problem to considering the evolution of a single vertical long-wave mode which is regular to the leading order and has an explicit analytic presentation. To investigate how the weak nonlinearity or/and viscosity affect the slow evolution of this mode represents a challenging, but not hopeless, task which will be dealt with in the subsequent papers of this series.

The authors are grateful to J. Healey for the helpful comments on the first draft of the paper. The work was supported by Forbairt Basic Research Grant SC-98-530, by INTAS (Grant 97-575, 01-234), by Grant HEA PRLT1 (501-133-2889) and by Institute for Nonlinear Science (Cork, Ireland).

Appendix. Evaluation of the Green function integral by the saddle point method

In §4 our analysis of the long-time asymptotics of the evolution of arbitrary perturbations has been reduced to evaluation of integrals of the type

$$\int_0^\infty \mathrm{e}^{\Phi(K;X,t)}\,\mathrm{d}K \tag{A 1}$$

We evaluate the integrals by the saddle point method adjusted for our problem by employing the version described in e.g. Wong (1989, §3), and Fedoryuk (1977) which is not commonly used. We provide below the key details of the analysis.

A.1. *Study of* I_0

Since all integrals I_n can be expressed as derivatives of I_0 ($I_n = \partial_x^n I_0$) we confine our analysis to I_0.

A.1.1. *Saddle points*

Consider the exponent of the integrand (4.15)

$$I_0 = \frac{1}{2\pi t^{1/2}} \int_0^\infty \mathrm{e}^{\Phi(K)}\,\mathrm{d}K + \text{c.c.}, \qquad \Phi(K) = \mathrm{i}KX + \mathrm{i}K^2 - \varkappa K^3 t^{-1/2}. \tag{A 2}$$

To find its saddle points we, in the standard manner, first look for the roots of its first derivative

$$\Phi'(K) = 0 \Rightarrow K_s^{\pm} = \frac{-1 \pm \sqrt{1 - X(3\mathrm{i}\varkappa t^{-1/2})}}{(3\mathrm{i}\varkappa t^{-1/2})}.$$

Since the integrals are concerned only with the QM part of the perturbation, which due to the Landau damping is important only in the zone $|X| \lesssim t^{1/6}$ determined by virtue of (4.20), in our context this means that $|X|\, t^{-1/2} \ll 1$ and for large t the roots can be approximated as follows:

$$K_s^{+} \cong -\tfrac{1}{2}X - \frac{3\varkappa\mathrm{i}}{8}\frac{X^2}{t^{1/2}} + O(t^{-1}), \quad K_s^{-} \cong \frac{2\mathrm{i}}{3\varkappa}t^{1/2} + \tfrac{1}{2}X + O(t^{-1/2}). \tag{A 3}$$

It is easy to see that the root K_s^{-} yields an exponentially small integrand and, therefore, the contribution due to the saddle point K_s^{-} can be neglected in our asymptotic study. Below we consider only the root K_s^{+} and omit superscript $+$.

Now we can find an approximation of $\Phi(K)$ in the saddle point K_s for large t:

$$\Phi_s \equiv \Phi(K_s) \cong -\frac{\mathrm{i}}{4}X^2 + \frac{\varkappa}{8}\frac{X^3}{t^{1/2}} + O(t^{-1}).$$

We introduce a new auxiliary independent variable $s(K)$, such that $\Phi(K) = -s^2 + \Phi_s$, i.e.

$$s^2 = \Phi_s - \Phi \cong -\mathrm{i}\left(K + \frac{X}{2}\right)^2 + \frac{\varkappa}{t^{1/2}}\left(K^3 + \frac{X^3}{8}\right) + O(t^{-1}). \tag{A 4}$$

If $K \to +\infty$, then $s \to \sqrt{\varkappa K^3 t^{-1/2}}$, which is real. It must be positive to ensure decay of the integrand. Therefore we take the branch of $s(K)$ which is positive for large positive K. Function $s(K)$ is given by

$$s \cong \sqrt{-\mathrm{i}\left(K + \frac{X}{2}\right)^2 + \frac{\varkappa}{t^{1/2}}\left(K^3 + \frac{X^3}{8}\right) + O(t^{-1})} \tag{A 5}$$

and is uniquely defined on the K-plane with cuts drawn from the branch point of $s(K)$:

$$K_b = -\tfrac{1}{2}X + o(t^{-1/2}) \tag{A 6}$$

towards $\pm\mathrm{i}\infty$, respectively.

To accomplish the $s(K)$ change of variables consider the limits of integration. When the upper limit holds, we find image s_0 of the boundary point ($K = 0$) on the s-plane:

$$s_0^2 = \Phi_s = -\frac{\mathrm{i}}{4}X^2 + \frac{\varkappa}{8}\frac{X^3}{t^{1/2}} + O(t^{-1}), \tag{A 7}$$

$$s_0 \cong \frac{1}{2\sqrt{\mathrm{i}}}X\sqrt{1 + \frac{\mathrm{i}\varkappa}{2}\frac{X}{t^{1/2}}} \cong \frac{X}{2\sqrt{\mathrm{i}}} + \frac{\varkappa\sqrt{\mathrm{i}}}{8}\frac{X^2}{t^{1/2}} + O(t^{-1}). \tag{A 8}$$

Hereinafter we use $\sqrt{\mathrm{i}} = \mathrm{e}^{\mathrm{i}\pi/4}$. Now integral (A 2) takes the form

$$I_0 = \frac{1}{2\pi t^{1/2}}\left\{\mathrm{e}^{s_0^2}\int_{s_0}^{+\infty}\mathrm{e}^{-s^2}K'(s)\,\mathrm{d}s + \text{c.c.}\right\}.$$

Notice that the directions $s \to +\infty$ as well as $K \to +\infty$ correspond to the direction of steepest decent of the phase function Φ.

To find $K'(s)$ we expand $K(s)$ and $K'(s)$ into series with respect to t^{-1} in the vicinity of the saddle point.† Let $K = K_s + \delta$ then, taking into account that $\Phi'_s = 0$, we have

$$s^2 \equiv \Phi_s - \Phi(K) = -\frac{\Phi''_s}{2}\delta^2 - \frac{\Phi'''_s}{3!}\delta^3 + \cdots.$$

Solving this equation with respect to δ by subsequent approximations assuming s to be small, we obtain

$$K = K_s + \sqrt{\frac{2}{-\Phi''_s}}s + \frac{\Phi'''}{3(\Phi''_s)^2}s^2 + \frac{3\Phi''''_s\Phi''_s - 5(\Phi'''_s)^2}{\sqrt{-2\Phi''_s}(\Phi''_s)^2}s^3 + \cdots.$$

In our case we have

$$\Phi''_s \cong 2\mathrm{i} + 3X\varkappa t^{-1/2} + O(t^{-1}) \quad (\sqrt{-\Phi''_s/2} \cong -1/\sqrt{\mathrm{i}} + (3/2)\varkappa\sqrt{\mathrm{i}}Xt^{-1/2} + O(t^{-1})),$$

$$\Phi'''_s = -6\varkappa t^{-1/2}, \qquad \Phi''''_s = 0.$$

Thus we arrive at the double series for $K(s; X, t)$

$$K \cong \left[-\tfrac{1}{2}X - \frac{3\varkappa\mathrm{i}}{8}\frac{X^2}{t^{1/2}} + O\left(\frac{1}{t}\right)\right] + \left[\sqrt{\mathrm{i}} - \frac{3\varkappa}{4\sqrt{\mathrm{i}}}\frac{X}{t^{1/2}} + O\left(\frac{1}{t}\right)\right]s + \left[\frac{\varkappa}{t^{1/2}} + O\left(\frac{1}{t}\right)\right]\frac{s^2}{2} + \cdots$$

and, differentiating term by term, we find

$$K' \cong \left[\sqrt{\mathrm{i}} - \frac{3\varkappa}{4\sqrt{\mathrm{i}}}\frac{X}{t^{1/2}} + O\left(\frac{1}{t}\right)\right] + \left[\frac{\varkappa}{t^{1/2}} + O\left(\frac{1}{t}\right)\right]s + \cdots.$$

Finally we obtain the integral

$$I_0 = \frac{1}{2\pi t^{1/2}}\mathrm{e}^{s_0^2}\int_{s_0}^{+\infty}\left[\sqrt{\mathrm{i}} + \frac{\varkappa}{t^{1/2}}\left(-\frac{3X}{4\sqrt{\mathrm{i}}} + s\right) + O\left(\frac{1}{t}\right)\right]\mathrm{e}^{-s^2}\,\mathrm{d}s + \text{c.c.}., \tag{A 9}$$

which can be integrated explicitly term by term. Note that for an arbitrary generic spectrum of $\hat{u}_0(k, 0)$ we can present the integrand as

$$\hat{u}_0\left(-\frac{1}{2}\frac{X}{t^{1/2}} + \frac{\sqrt{\mathrm{i}}}{t^{1/2}}s + O\left(\frac{1}{t}\right), 0\right) \times \left[\sqrt{\mathrm{i}} + \frac{\varkappa}{t^{1/2}}\left(-\frac{3X}{4\sqrt{i}} + s\right) + O\left(\frac{1}{t}\right)\right]\mathrm{e}^{-s^2}.$$

A.1.2. *Main term of the asymptotics*

The main term of (A 9) we were looking for and its first-order correction ΔI_0, which is needed to estimate the accuracy, can both be expressed in terms of error

† Strictly speaking, to obtain uniform asymptotics of I_0 (i.e. for all X) we should expand $K(s)$ into a series which approximates $K(s)$ simultaneously at the two points, the saddle point ($s = 0$) and the boundary point (s_0). The corresponding expansion takes the form $K(s) = \sum_{n=0}^{\infty}(a_n + b_n s)s^n(s - s_0)^n$. Retaining N terms we can get exact values up to the Nth derivatives at the points 0 and s_0. However, it can be shown that for the case in hand this rigorous approach, compared for I_0 with the one-point expansion employed, results in a discrepancy only in the third term of the asymptotic series with respect to $t^{-1/2}$. Thus, for our purposes the rigorous cumbersome approach is unnecessary.

functions

$$I_0 \cong \mathrm{Re}\left[\frac{\sqrt{\mathrm{i}}}{2\sqrt{\pi}t^{1/2}}\,\mathrm{e}^{s_0^2}\,\mathrm{erfc}\,\{s_0\}\right] + O(t^{-1}), \tag{A 10}$$

$$\Delta I_0 \cong -\left[\mathrm{Re}\frac{3\varkappa}{8\sqrt{\pi}\sqrt{\mathrm{i}}}\frac{X}{t}\,\mathrm{e}^{s_0^2}\,\mathrm{erfc}\,\{s_0\}\right] + \frac{\varkappa}{2\pi t} + O\left(t^{-3/2}\right), \tag{A 11}$$

where $\mathrm{erfc}\,\{s_0\} = (2/\sqrt{\pi})\int_{s_0}^{+\infty}\mathrm{e}^{-s^2}\,\mathrm{d}s$ is the complementary error function (see Abramowitz & Stegun 1965).

A.1.3. *Large-negative-X asymptotics*

First we consider large negative X. Using the known asymptotic behaviour of the error function for large values of the real part of its argument (see Abramowitz & Stegun 1965), we find for $|X| \gg 1$ and $X < 0$:

$$I_0 \approx \frac{1}{\sqrt{\pi}t^{1/2}}\sin\left\{\frac{X^2}{4}+\frac{\pi}{4}\right\}\exp\left\{-\frac{\varkappa|X|^3}{8t^{1/2}}\right\} + \frac{2}{\pi t^{1/2}X^3} + O(t^{-1}). \tag{A 12}$$

The first term in (A 12) describes an oscillating pattern, which prevails for moderate $-X$: $1 \ll -X < O(t^{1/6})$ (i.e. in the QM zone) and decays very fast for greater $-X$.

The second summand describes the non-oscillatory part of the QM contribution. Its asymptotics in the non-scaled variables takes the form

$$\frac{2}{\pi t^{1/2}X^3} = \frac{2t}{\pi(x-t)^3} \sim t^{-2} \quad \text{for fixed } x \text{ (or } x/t) \text{ and } t \to \infty,$$

i.e. this component of the QM part decays faster than the 'initial transition' contribution. Nevertheless it is this term which determines the far asymptotics of I_0 behind the QM zone. For our analysis this term is not important although it contributes importantly to the integral $\int_{-\infty}^{+\infty} I_0(x,t)\,\mathrm{d}x$. In the accepted normalization this integral is equal to one for all t as its spatial spectrum $\exp\{\mathrm{i}k(x-t)+\mathrm{i}k|k|t-\varkappa k^2|k|t\}$ tends to unity when $k \to 0$.

A.1.4. *Simplified real formula for* I_0

If we look at (A 12) it is easy to see that for large $-X$ the value of I_0 is the product of the large-$|X|$ asymptotics for $I_0^{\varkappa=0}$ and the damping factor

$$\exp\left\{-\frac{\varkappa|X|^3}{8t^{1/2}}\right\} \equiv \exp\left\{-\varkappa\left(\frac{\Delta v}{2}\right)^3 t\right\}$$

plus a small non-oscillatory addend $\Delta I_{\text{non-osc.}}$:

$$I_0 \approx I_0^{\varkappa=0}\exp\left\{-\frac{\varkappa|X|^3}{8t^{1/2}}\right\} + \Delta I_{\text{non-osc}} + \cdots.$$

The addend $\Delta I_{\text{non-osc}}$ (which behaves as $2/(\pi t^{1/2}X^3)$ when $|X| \ll 1$), can be neglected in most plausible considerations.

On the other hand, for small and moderate $-X$ ($|X| \ll t^{1/6}$) the effect of the Landau damping is negligibly small

$$\exp\left\{-\frac{\varkappa|X|^3}{8t^{1/2}}\right\} \cong 1, \quad I_0 \cong I_0^{\varkappa=0},$$

i.e. $\Delta I_{\text{non-osc}} \to 0$ as $X \to 0$.

This observation suggests that a good approximation for I_0 might be

$$I_0 \cong I_0^{\varkappa=0} \exp\left\{\frac{\varkappa}{8}\frac{X^3}{t^{1/2}}\theta(-X)\right\}. \tag{A 13}$$

We would arrive at the same formula by applying the multiple-scale technique. Separating the scales and a seeking solution in the separable form, i.e. as a product of two functions depending on either the 'fast' or 'slow' scale variable, we obtain $I_0^{\varkappa=0}$ as the solution describing the dependence on the 'fast' variable, while the Landau damping factor describes the 'slow' dependence. Comparing the 'simplified' two-scale formula (A 13) with the more precise asymptotic formula (A 10) we found that the relative error is $O(10^{-2})$ for the times 10^2–10^3. We conclude that the 'simplified' formula (A 13) provides an accuracy sufficient for our purposes and will use it in our analysis throughout the paper.

A.2. *Study of* I_G

Now we consider a slightly modified integral which is central for the investigation of initially long-wave perturbations in § 4.3:

$$I_G = \frac{1}{2\pi t^{1/2}}\int_0^\infty \mathrm{e}^{\Phi_G(K)}\,\mathrm{d}K + \text{c.c.}, \tag{A 14}$$

$$\Phi_G(K) = \mathrm{i}KX + \mathrm{i}K^2 - \varkappa K^3 t^{-1/2} - KL^2 t^{-1}, \quad L \gg 1.$$

The difference compared to I_0 is in the last term, which is small when $t \to \infty$ but remains important for sufficiently large t due to the large parameter L. A straightforward expansion in large t misses the intermediate asymptotics we are interested in. This asymptotics occurs when the last two terms in (A 14) are of comparable smallness. To describe this situation in terms of asymptotic expansions we introduce temporarily a fictitious small parameter ε which reflects the smallness of the last two terms:

$$\Phi_G(K) = \mathrm{i}KX + \mathrm{i}K^2 - \varepsilon\varkappa K^3 t^{-1/2} - \varepsilon KL^2 t^{-1}. \tag{A 15}$$

We consider ε as a small parameter only temporarily and equate it to unity in the final results.

Solving equation $\Phi_G'(K) = 0$ by successive approximations we find the saddle point

$$K_s \cong -\tfrac{1}{2}X - \varepsilon\frac{3\varkappa\mathrm{i}}{8}\frac{X^2}{t^{1/2}} + \varepsilon\frac{\mathrm{i}L^2}{2}\frac{X}{t} + O(\varepsilon^2).$$

By substituting $K = K_s$ into (A 15) we evaluate $\Phi_G(K)$ at the saddle point K_s:

$$\Phi_{s,G} \cong -\frac{\mathrm{i}}{4}X^2 + \varepsilon\frac{\varkappa}{8}\frac{X^3}{t^{1/2}} - \varepsilon\frac{L^2}{4}\frac{X^2}{t} + O(\varepsilon^2).$$

Similarly to § A.1, a substitution $s(K)$, such that $\Phi_G(K) = -s^2 + \Phi_{s,G}$, yields

$$s^2 \cong -\mathrm{i}\left(K + \frac{X}{2}\right)^2 + \varepsilon\frac{\varkappa}{t^{1/2}}\left(K^3 + \frac{X^3}{8}\right) + \varepsilon\frac{L^2}{t}\left(K^2 - \frac{X^2}{4}\right). \tag{A 16}$$

If $K \to +\infty$, then $s \to \sqrt{\varepsilon\varkappa K^3 t^{-1/2}/8}$ which is real. As in § A.1 we choose the appropriate branch of $s(K)$ which is positive for large positive K:

$$s \cong \sqrt{-\mathrm{i}\left(K + \frac{X}{2}\right)^2 + \varepsilon\left[\frac{\varkappa}{t^{1/2}}\left(K^3 + \frac{X^3}{8}\right) + \frac{L^2}{t}\left(K^2 - \frac{L^2}{4}\right)\right]}. \tag{A 17}$$

The function is uniquely defined on the K-plane with cuts drawn from the branch point of $s(K)$:

$$K_b \cong -\tfrac{1}{2}X + o(\varepsilon) \tag{A 18}$$

towards $\pm\mathrm{i}\infty$, respectively.

We find image of the boundary point ($K = 0$) on the s-plane:

$$s_{0,G} \cong \frac{X}{2\sqrt{\mathrm{i}}} + \varepsilon\frac{\varkappa\sqrt{\mathrm{i}}}{8}\frac{X^2}{t^{1/2}} - \varepsilon\frac{L^2\sqrt{i}}{4}\frac{X}{t}, \tag{A 19}$$

$$s_{0,G}^2 = \Phi_s \cong -\frac{\mathrm{i}}{4}X^2 + \varepsilon\frac{\varkappa}{8}\frac{X^3}{t^{1/2}} - \varepsilon\frac{L^2}{4}\frac{X^2}{t}. \tag{A 20}$$

The main term of (A 9) is

$$I_G \cong \mathrm{Re}\frac{\sqrt{\mathrm{i}}}{2\sqrt{\pi}t^{1/2}}\,\mathrm{e}^{s_{0,G}^2}\,\mathrm{erfc}\,\{s_{0,G}\}\bigg|_{\epsilon=1} + O(t^{-1}).$$

In our analysis we use a more useful simplified real formula for I_G, obtained in the same manner as in § A.1:

$$I_G = I_0^{\varkappa=0}\exp\left\{\left(\frac{\varkappa}{8}\frac{X^3}{t^{1/2}} - \frac{L^2}{4}\frac{X^2}{t}\right)\theta(-X)\right\}. \tag{A 21}$$

REFERENCES

Abramowitz, M. & Stegun, I. A. 1965 *Handbook of Mathematical Functions*. Dover.

Bowles, R. G. A. & Smith, F. T. 1995 Short-scale effects on model boundary-layer spots *J. Fluid Mech.* **295**, 395–407.

Briggs, R. J., Daugherty, J. D. & Levy, R. H. 1970 Role of Landau damping in crossed-field electron and inviscid shear flow. *Phys. Fluids* **13**, 421–432.

Case, K. M. 1960 Stability of inviscid plane Couette flow. *Phys. Fluids* **3**, 143–148.

Chandrasekhar, S. 1981 *Hydrodynamic and Hydromagnetic Stability*. Dover.

Dickey, L. A. 1960 Stability of plane-parallel flows of an ideal fluid. *Dokl. Akad. Nauk SSSR* **125**(5), 1068–1071; Engl. translation: *Sov. Phys. Doclady* **5**, 1179–1182.

Dickey, L. A. 1976 *Hydrodynamic Stability and Atmosphere Dynamics*. Gidrometeoizdat, Leningrad (in Russian).

Drazin, P. G. & Reid, W. H. 1981 *Hydrodynamic Stability*. Cambridge University Press.

Dupont, R. & Caulliez, G. 1993 Caractérisation de la couche limite laminaire générée par le vent sous une interface air-eau. In: *Actes du 11é Congres Français de Mecanique*, vol. 3, pp. 257–260. Association Universitaire de Mécanique.

Falkner, V. M. & Skan, S. W. 1931 Solutions of boundary-layer equations. *Phil. Mag.* **2**, 865–896.

Fedoryuk, M. V. 1977 *The Saddle Point Method*. Nauka, Moscow (in Russian).

Jacobs, R. G. & Durbin, P. A. 2001 Simulations of the bypass transition. *J. Fluid Mech.* **428**, 185–212.

Kelbert, M. Ya. & Sazonov, I. A. 1996 *Pulses and Other Wave Process in Fluids*. Kluwer.

Landau, L. D. 1946 On the oscillation of the electronic plasma. *J. Phys. USSR* **10**, 25.

Lin, C. C. 1955 *The Theory of Hydrodynamic Stability*. Cambridge University Press.

Reznik, G. M. Zeitlin, V. & Ben Jelloul, M. 2001 Nonlinear theory of geostrophic adjustmnt. I. Rotating shallow water model. *J. Fluid Mech.* **445**, 93–120.

Rossby, C.-G. 1937 On the mutual adjustment of pressure and velocity distributions in certain simple curent systems. I. *J. Mar. Res.* **1**, 15–28.

Rossby, C.-G. 1938 On the mutual adjustment of pressure and velocity distributions in certain simple curent systems. II. *J. Mar. Res.* **1**, 239–263.

Saffman, P. G. 1994 *Vortex Dynamics*. Cambridge University Press.

Schmidt, P. J & Henningson, D. S. 2001 *Stability and Transition in Fluid Flows*. Springer.

Shrira, V. I. 1989 On the 'subsurface' waves in the oceanic upper mixed layer. *Dokl. Akad. Nauk SSSR* **308**, 732–736; Engl. translation: *Trans. (Dokl.) USSR Acad. Sci., Earth Sci.* **308**, 276–279.

Shrira, V. I. & Sazonov, I. A. 2001 Quasi-modes in boundary-layer-type flows. Part 1. Inviscid two-dimensional spatially harmonic perturbations. *J. Fluid Mech.* **446**, 133–171.

Smith F. T. 1982 On the high Reynolds number theory of laminar flows *IMA J. Appl. Maths* **28**, 207–281.

Smith, F. T., Dodia, B. T. & Bowles, R. G. A. 1994 On global and internal dynamics of spots: a theoretical approach *J. Engng Maths* **28**, 73–91.

Trefethen, L. N., Trefethen, A. E, Reddy, S. C. & Driscoll, T. A. 1993 Hydrodynamic stability without eigenvalues. *Science* **261**, 578–584.

Wong, R. 1989 *Asymptotic Approximations of Integrals*. Academic.